# A review on anode on-cell catalyst reforming layer for direct methane solid oxide fuel cells

Peng Qiu<sup>1</sup>, Shichen Sun<sup>2</sup>, XinYang<sup>2</sup>, Fanglin Chen<sup>2\*</sup>, Chunyan Xiong<sup>3</sup>, Lichao Jia<sup>3\*</sup> and Jian Li<sup>3</sup>

- <sup>1</sup> School of Materials Science and Engineering, Shandong University of Science and Technology, Qingdao, 266590, China
- <sup>2</sup> Department of Mechanical Engineering, University of South Carolina, Columbia, SC, 29208, United States; Email address: chenfa@cec.sc.edu
- <sup>3</sup> Center for Fuel Cell Innovation, School of Materials Science and Engineering, State Key Lab of Material Processing and Die & Mound Technology, Huazhong University of Science and Technology, Wuhan, 430074, China; Email address: jialc@hust.edu.cn

#### **Abstract**

The commercialization of solid oxide fuel cells (SOFCs) can be significantly promoted with the direct utilization of methane, which is the primary component in natural gas and the second most abundant anthropogenic greenhouse gas. However, carbon deposition on most commonly used Ni-based anode is the bottle-necking issue inhibiting long-term stability of direct methane SOFCs. To avoid such a problem, methane is typically reformed (internally or externally) in SOFCs. Consider the cost, system simplification, coking resistance, and material selection, the on-cell catalytic reforming layer (OCRL) is one of the most promising designs for direct methane SOFCs. Reforming catalytic materials are typically consisted of active component, substrate and catalytic promoter, all of which have a significant impact on the catalytic activity, sintering resistance and coking resistance of methane reforming catalysts. This review summarizes the influence of the various components, some common OCRL materials used, their applications in direct methane SOFCs, reforming and coking resistance mechanism, and the remaining challenges. The effective utilization of OCRL plays a pivotal role in promoting the development of direct methane SOFCs and the commercialization of SOFCs.

**Keywords**: methane, solid oxide fuel cells, Ni-based anode, coking resistance, on-cell catalytic reforming layer

#### 1. Introduction

As the world-wide energy demands increase dramatically with rapid economic development and population growth in the past decades, the development and utilization of various new energy sources such as solar energy, wind energy, nuclear energy, hydropower and other renewable energies have become research focus in recent years [1-3]. However, the share of these new energy sources in total energy consumption is still low and limited by many factors, especially immature technology development, site limitations, and the supply stability. Thus, the dominant proportion of energy consumption is still rely on traditional fossil energy sources such as coal, petroleum, and natural gas [4], which could lead to serious environmental pollution when direct combustion is adopted. In addition, due to the limitation of the Carnot cycle, direct combustion will cause a large amount of energy loss during operation [5]. Thus, developing clean and efficient ways of utilizing fossil energy sources has great significance from both economic and environment considerations.

Solid oxide fuel cell (SOFC) is an energy conversion device that can electrochemically converting the chemical energy in fossil fuels, biomass fuels or other hydrocarbon fuels into electricity. Advantages such as broad fuel options, high efficiency, low emissions, and low noise make SOFCs a promising technology for application of distributed power stations, backup power sources, as well as transportation and portable applications [6-9]. As a comprehensive consideration of cost, mechanical strength, performance and other factors, the most commonly used single cells in SOFC stacks are Ni-based anode supported single cells [10]. When directly feeding with hydrocarbon fuels, however, the severe carbon deposition on Ni-based anode is fatal to the long-term stable operation of SOFC stacks. Reforming hydrocarbon fuels into syngas before feeding to the anode of SOFC is an effective method to prevent carbon deposition on Ni-based anode [11]. Thus, fuel reforming technology becomes critical for efficient utilization of hydrocarbon fuels in SOFCs [12-14], and can eventually promote the commercialization of SOFCs. On-cell catalytic reforming layer (OCRL) is regarded as the most promising methane reforming design

for direct methane SOFCs considering cost, simplified system, coking resistance, and options for material selection. In this review, a detailed summary of material selections, applications, reforming and coking resistance mechanism, challenges and future prospective of OCRL is provided.

# 1.1 Ni-based anode supported SOFCs

SOFC single cell is composed of porous cathode, porous anode and dense electrolyte sandwiched between two electrodes. Based on the types of charge carrier in the electrolyte, SOFC can be generally divided into oxide-ion (O<sup>2-</sup>) conducting SOFC (O-SOFC) and proton (H<sup>+</sup>) conducting SOFC (H-SOFC). Obviously, these two types of SOFC have different working principles, as shown in **Figure 1**. In O-SOFC, oxygen undergoes oxygen reduction reaction (ORR) in the cathode, and the generated O<sup>2-</sup> are directionally transmitted from the cathode to the anode through the dense electrolyte. O<sup>2-</sup> will then react with the fuel gas (e.g. H<sub>2</sub> or methane) at the three-phase boundary (TPB) of the anode, generating electricity, H<sub>2</sub>O and other products. For H-SOFC, the charge carriers conducted by the electrolyte are H<sup>+</sup> instead of O<sup>2-</sup>. The fuel gas (e.g. H<sub>2</sub>) undergoes oxidation reaction and generates H<sup>+</sup> in the anode. The generated H<sup>+</sup> will then be directionally transmitted to the cathode side through the electrolyte, generating electricity and H<sub>2</sub>O by combining with O<sup>2-</sup> generated in the cathode.

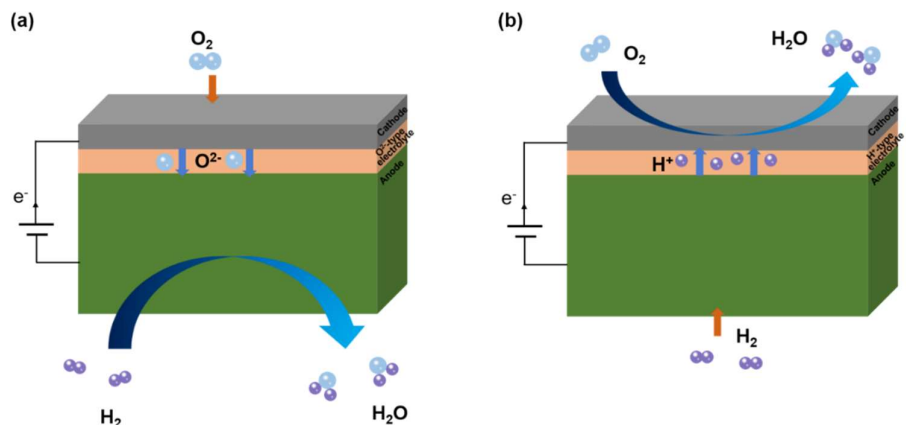


Figure 1 Schematic diagram of the working principle of O-SOFC (a) and H-SOFC (b).

The state-of-the-art cell configuration applied in SOFC stacks is anode supported single cells [15]. Compared to electrolyte supported single cells which typically has

high ohmic resistance due to the thick electrolyte layer, anode supported single cells generally has lower overall cell resistance, which mainly comes from the electrolyte and the cathode [16, 17]. By applying thin cathode and electrolyte layers, the operating temperature of anode support single cells can be significantly reduced to the intermediate temperature range (600~750 °C) compared to electrolyte support cells which are typically operated above 800°C. The reduced operating temperature can thus benefit the commercialization of the SOFCs by significantly reducing the cost and improving the durability of SOFC system [18]. At present, Ni-based cermet composites are widely adopted as the anode materials in most mature and advanced SOFC technologies [17, 19, 20]. The low cost, high electronic conductivity and electrochemical catalytic activity for the anode reaction makes Ni the most attractive material as the anode of SOFCs. The second phase material for cermet anode is usually chosen to be the electrolyte material, for the purpose of providing high ionic conductivity or proton conductivity for anode reaction as well as reducing thermal expansion mismatch between anode and electrolyte layers. Moreover, the electrolyte materials in cermet anode also act as the mechanical support and prevention for possible coarsening of Ni particles during operation.

#### 1.2 Fuels challenges in SOFCs

SOFCs have a wide range of fuel options. Among them, H<sub>2</sub> is considered to be the ideal fuel for SOFCs mostly due to its environmentally friendliness with H<sub>2</sub>O as combustion product. Common ways for the industry to produce H<sub>2</sub> are electrolysis, hydrocarbon steam reforming, hydrocarbon cracking, and water gas conversion, etc. H<sub>2</sub> has a wide range of applications in industry, such as chemical synthesis, oil refining, electronics, metal processing, *etc.* [21]. Recently, global demand for H<sub>2</sub> has greatly surged due to the strict environmental protection requirement. Despite of the broad prospects, some major barriers remain for the application of H<sub>2</sub> energy such as production costs, storage, transportation and technological uncertainty [22]. In addition to H<sub>2</sub>, hydrocarbons such as natural gas and biogas can also be adopted as fuel for SOFCs [23]. Compared to H<sub>2</sub>, hydrocarbon fuels are readily available in most area, and

possess several other advantages such as lower cost for production, storage and transportation. In fact, the capability of utilizing hydrocarbon fuels makes SOFCs attractive in many applications when H<sub>2</sub> is not available or hard to obtain. The main approach to utilize hydrocarbon fuels for SOFC is to convert hydrocarbon fuels into syngas through fuel reforming.

Methane is the simplest hydrocarbon fuel and the primary component of natural gas and biogas. Its wide range of sources and low price make it extremely appealing in SOFCs. Recently, there have been extensive studies on direct methane SOFCs, which will also be summarized in this review.

The research on the direct use of biomass oil as SOFC fuel is still in its infancy. Biomass oils such as methanol, formic acid, isooctane[24] and biodiesel[25] could be reformed into gas mixture composed of H<sub>2</sub>, CO, CH<sub>4</sub>, etc., which can be used by SOFCs. Biomass oil made from animal oil and vegetable oil has the following advantages when used as the fuel for SOFC: (1) biomass oil can replace some fossil fuels and help alleviate the greenhouse effect; (2) biomass oil contains oxygen, which can alleviate carbon deposition on SOFC anode; (3) biomass oil is renewable and has a wide range of sources; (4) biomass oil has high ignition point and therefore high safety; and (5) biomass oil is easily biodegradable and environmentally friendly. Despite of the above advantages of biomass oil, its calorific value is lower than that of hydrogen and hydrocarbon fuels. Biomass oil is composed of combustible matter, inorganic matter and moisture. The higher the content of inorganic matter and moisture, the lower the calorific value. Since the relative content of hydrogen and carbon elements in biomass oil is lower than that the corresponding hydrogen and hydrocarbon fuels, its energy density is also lower. In addition, problems such as carbon deposition on catalyst and high impurity content of biomass oil cannot be ignored [26].

## 1.3 Carbon deposition for SOFCs using Ni-based anode

While the Ni-based anode has excellent catalytic oxidation performance towards hydrocarbon fuel, it can also catalyze the direct cleavage of C-H bonds, thereby leading to serious carbon deposition. The deposited carbon will grow up in the form of carbon

nanofibers or nanotubes on Ni particles, which is gradually enveloped and lose catalytic activity, along with serious degradation of cell performance [21, 27-29]. Some perovskite oxides have outstanding reforming catalytic performance, but their ability to catalyze oxidation and cleavage of C-H bonds is rather weak [30-32]. Nevertheless, based on the comprehensive consideration of cost, fabrication simplicity, and electrochemical performance, Ni-based anode are still the best choice for commercial SOFC stacks. Thus, solving the issue of carbon deposition for Ni-based anodes become crucial to the development of direct hydrocarbon SOFCs.

Extensive efforts have been made to solve the problem of carbon deposition in recent years, and some effective strategies have been successfully developed. Figure 2 shows several representative strategies used in Ni-based anode supported SOFCs for direct hydrocarbon utilization. One of the common strategies to alleviate carbon deposition is to add large amounts of steam into hydrocarbon fuel stream and achieve a high steam to carbon ratio (S/C) larger than 2 [33, 34]. In addition to steam, CO<sub>2</sub> can also be used to dry reform hydrocarbon fuel into syngas to alleviate carbon deposition [35, 36]. Moreover, lowering the operating temperature is also an alternative option. It has been reported that deposited carbon is not thermodynamically stable at the temperature range of 550 to 650 °C [37], as thermal cracking of CH<sub>4</sub> to carbon and H<sub>2</sub> is inhibited below 650 °C, while the disproportionation reaction of CO to carbon and CO<sub>2</sub> is thermodynamically unfavorable above 550 °C. Although it can effectively alleviate carbon deposition, the reduction in operating temperature is often not favorable due to the accompanying lower cell power output and fuel utilization. Moreover, carbon deposition can also be suppressed by so-called "self de-coking" reaction in O-SOFC. Such reaction is achieved by supplying sufficient oxide ion to react with deposited carbon under high current loading which can accelerate the transportation of oxide ions towards the anode reaction sites [38]. However, the excess oxide ions in this case are limited to the electrochemical active area of the anode, typically within ~10 µm distance from the electrolyte. For anode supported SOFCs, carbon deposition could occur on much wider areas of the anode which could not be reached by  $O^{2}$ .

The second strategy, as shown in **Figure 2b**, is to alleviate carbon deposition by the addition of nano-catalysts in the anode support. Precious metals such as Pd[39, 40] and Ru[41, 42] are commonly used as the catalyst. The addition of precious metals promotes the electrochemical oxidation reaction of hydrocarbon fuels, and improves the carbon deposition resistance of Ni. Transition metals such as Cu[43], Co[44, 45], Fe[46] are also widely used as additives, but the role of these metal elements is to reduce the catalytic activity of Ni towards carbon deposition by forming an alloy with Ni. Similarly, some metal oxides are also used as modified materials in Ni-based anode, such as CeO<sub>2</sub> and doped CeO<sub>2</sub> [21, 27-29, 47-49]. They have variable valences under reducing atmosphere, and excellent catalytic activity toward reforming reactions. Some alkaline earth metal oxides, such as CaO[50] and BaO[51], are also reported to have the capability of enhancing the self de-coking ability of Ni-based anode.

In the third strategy, as shown in **Figure 2c**, a (Y, Ce)O<sub>2- $\delta$ </sub> (YDC) interlayer is applied between anode and electrolyte, and the following advantages are obtained [52]. Firstly, YDC transforms into a mixed ionic-electronic conductor (MIEC) under reducing atmosphere, increasing the reactive area of anode beyond TPB. Secondly, the high ionic conductivity of YDC can help effective conduction of O<sup>2-</sup> from the electrolyte to the anode. Thirdly, the high oxygen vacancies of YDC can store O<sup>2-</sup> and promote the oxidation of hydrocarbon fuel. Finally, YDS is known to have good dry reforming ability and resistance to carbon formation [53, 54]. However, the high co-sintering temperature of the anode-supported single cell will reduce the ability of YDC to release lattice oxygen ions [53].

For the last strategy, as shown in **Figure 2d**, a porous OCRL is applied on the anode support. Before the hydrocarbon fuel enters the anode, it undergoes a reforming reaction under the catalysis of the OCRL and is converted into syngas, during which the carbon deposition could be greatly reduced. Compared with other strategies, the addition of OCRL can alleviate carbon deposition more effectively, and the reforming reaction can make full use of the heat released by electrochemical oxidation. However, OCRL may have an adverse effect on mass transport, and its porosity needs to be optimized. More

detailed information about this strategy will be given in the rest of this review, especially on the application of OCRL against carbon deposition for Ni-based anode supported SOFCs when directly fed with hydrocarbon fuel.

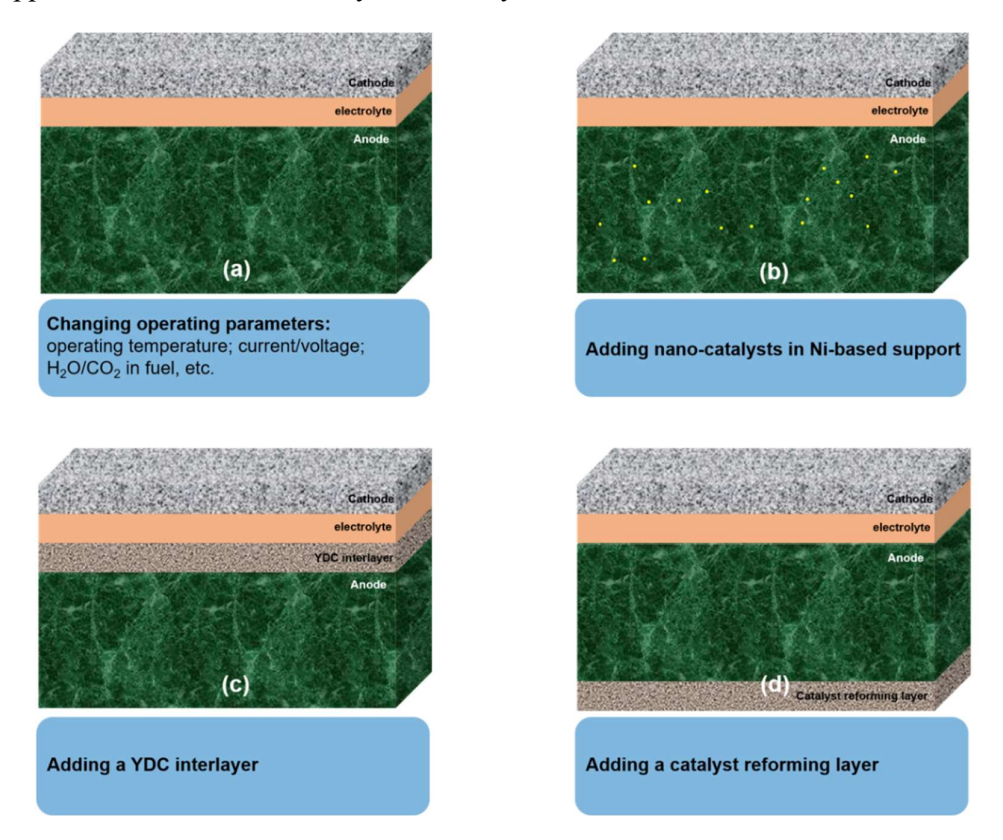


**Figure 2** The strategies used in Ni-based anode supported SOFCs for direct hydrocarbon utilization.

## 1.4 Fuel reforming in SOFCs

The fuel reforming reactions in SOFC systems are important when hydrocarbon fuels were adopted. These reactions can be conducted both externally and internally. The external reforming utilizes a fuel reformer independent of the SOFC stack, in which the hydrocarbon fuel is first reformed into syngas in the external reformer prior to entering the anode of SOFCs. Such fuel reformer needs extra stream or CO<sub>2</sub> to reform hydrocarbon fuel. Some obvious drawbacks exist for the external reforming technology. Firstly, the independent reformer is required as an additional component, which increases design difficulty and cost for the SOFC stack. Secondly, as a highly endothermic reaction, fuel reforming requires extra heat for the reformer, which

increases total energy consumption and reduce the overall system efficiency. Furthermore, excess air flow beyond stoichiometric amount is required to ensure that the SOFC stack does not overheat [55]. Moreover, for external reforming technology, especially steam reforming, the corrosion of fuel pipelines is also a serious problem. However, as far as the current level of technology is concerned, external reforming is still the main reforming method for commercial SOFCs.

The internal reforming is conducted by placing the fuel reforming inside the SOFC stack, so that no external reformer is needed. Its unique advantages include simplified system design without external reformer, and reduced air flow because the heat released by the anode reaction can also be used for the reforming reaction [55]. In addition, since the anode electrochemical oxidation can produce steam or CO<sub>2</sub>, less additional stream or CO<sub>2</sub> is needed for internal reforming [56]. Internal reforming can be divided into direct internal reforming and indirect internal reforming. Direct internal reforming occurs directly inside the SOFC anode, which requires the SOFC anode to possess dual functions of catalyzing the fuel reforming reaction and the fuel electrochemical oxidation reaction. Different from direct internal reforming, indirect internal reforming separates the reaction sites for fuel reforming from that for fuel electrochemical oxidation. The fuel reforming reaction takes place in the gas channel before entering the anode, and the anode only needs to have excellent electrochemical oxidation catalytic performance. Thus, indirect internal reforming has much more flexible choice for reforming catalyst and anode material, with fewer restrictions on compromising among each other. OCRL in SOFC is a typical design for the indirect internal reforming strategy and will be elaborated in detail in this review.

## 2. Methane conversion in Ni-based anode

Methane, the simplest hydrocarbon fuel and the most abundant organic compound on the planet, is the main component in natural gas and easily obtained from industrial production. Direct or indirect utilization of methane in SOFCs can overcome many obstacles accompanied with ordinary SOFC fuel H<sub>2</sub>, such as high cost of production, compression and transportation. The most important step for utilizing methane is the

methane conversion in SOFC, thus understanding the conversion mechanism of methane in SOFCs is the basis for realizing direct methane SOFCs in power generation. The conversion of methane in Ni-based anode is a combination of multiple reactions rather than a single reaction, and usually includes the following reactions.

Electrochemical oxidation:

$$CH_4 + O^{2-} \rightarrow 2H_2 + CO + 2e^-$$
 (1)

$$CH_4 + 20^{2-} \rightarrow H_2 + CO + H_2O + 4e^-$$
 (2)

$$CH_4 + 20^{2-} \rightarrow 2H_2 + CO_2 + 4e^-$$
 (3)

$$CH_4 + 30^{2-} \rightarrow H_2 + H_2O + CO_2 + 6e^-$$
 (4)

$$CH_4 + 30^{2-} \rightarrow 2H_2O + CO + 6e^-$$
 (5)

$$CH_4 + 40^{2-} \rightarrow 2H_2O + CO_2 + 8e^-$$
 (6)

Steam reforming:

$$CH_4 + H_2O \to CO + 3H_2$$
 (7)

Dry reforming:

$$CH_4 + CO_2 \to 2CO + 2H_2$$
 (8)

Decomposition:

$$CH_4 \to C + 2H_2 \tag{9}$$

Direct electrochemical oxidation of methane (Eq 1~6) is difficult to achieve for Nibased anode. Both theoretical and experimental studies believe that the largest energy barrier in the path is caused by the initial rupture of the first C-H bond [55]. It's worth mentioning that for direct methane SOFCs, methane oxidation reactions are usually accompanied by direct decomposition of methane (Eq 9), leading to serious carbon deposition and performance degradation. In addition, the oxidation products (H<sub>2</sub>O and CO<sub>2</sub>) from Eq 1~6 will also react with methane following Eq 7&8.

Steam reforming of methane (SRM, Eq 7) is currently the main means for industrial production of H<sub>2</sub>. It is reported that more than 80% of H<sub>2</sub> in the world has been produced in SRM [57]. SRM is usually carried out at a high temperature of 800~1000 °C with a high pressure of 35 bar in the presence of a Ni-based catalyst. The main reaction, as shown in Eq (8), usually coexists with the water-gas shift (WGS) reaction shown in Eq

(10) [58]. The SRM product CO can increase the H<sub>2</sub> concentration in the syngas through WGS, while converting most of CO into CO<sub>2</sub>. As a result, methane is converted primarily to H<sub>2</sub> for ease of electrochemical oxidation in the SOFCs and to obtain high performance [55].

$$CO + H_2O \to CO_2 + H_2$$
 (10)

CO<sub>2</sub> reforming of methane is also called dry reforming of methane (DRM, Eq 8). It is a catalytically induced process that produces syngas (mainly containing H<sub>2</sub> and CO) to be used as a sustainable fuel alternative to fossil fuel. Using the two major components (CH<sub>4</sub> and CO<sub>2</sub>) in biogas which is cheap and readily available, DRM presents huge economic benefits. Moreover, the utilization and conversion of CH<sub>4</sub> and CO<sub>2</sub> which are both greenhouse gases, is of great environmental significance. However, as an endothermic reaction, DRM requires high operating temperatures, usually in the range of 750~1000 °C, implying high energy consumption and thus high operating cost [59-61].

In addition, Ni has a strong ability to catalyze the direct cleavage of C-H bonds [62], so the catalytic decomposition of methane (CDM, Eq 9) is also a common methane conversion method in Ni-based anode. The products of CDM are H<sub>2</sub> and carbon. The former can be easily catalytic oxidized by Ni-based anode, while the latter is mainly deposited on the surface of Ni particles in the form of carbon fibers or carbon nanotubes, which is the main cause of carbon deposition on Ni-based anode. Therefore, it is necessary to avoid CDM as much as possible when fed with methane in SOFCs. It is worth noting that SRM and DRM may only occur when the temperature is higher than 600 °C, and the CO disproportionation reaction is unlikely to occur under this condition, as shown in **Figure 3**. The conversion of methane in the Ni-based anode mainly includes methane electrochemical oxidation, SRM, DRM and CDM when the operating temperature is higher than 600 °C, and coking mainly comes from CDM, as shown in **Figure 4a**. When the operating temperature of the SOFC is lower than 600 °C, the conversion of methane in the Ni-based anode is mainly electrochemical oxidation, and coking mainly comes from the CO disproportionation reaction.

When the operating temperature of the SOFC is higher than 600 °C, after the introduction of OCRL, methane is first subjected to DRM or SRM in the OCRL, as shown in **Figure 4b**. The reforming catalyst can convert methane into synthesis gas at a high conversion rate, and the concentration of methane entering the Ni-based anode is therefore substantially reduced, thereby alleviating the coking issue.

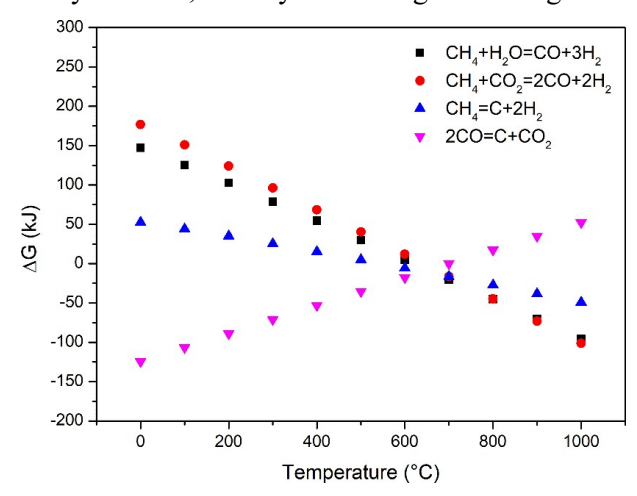


**Figure 3** Correspondence between Gibbs free energy and temperature for DRM, SRM, CDM and CO disproportionation reaction.

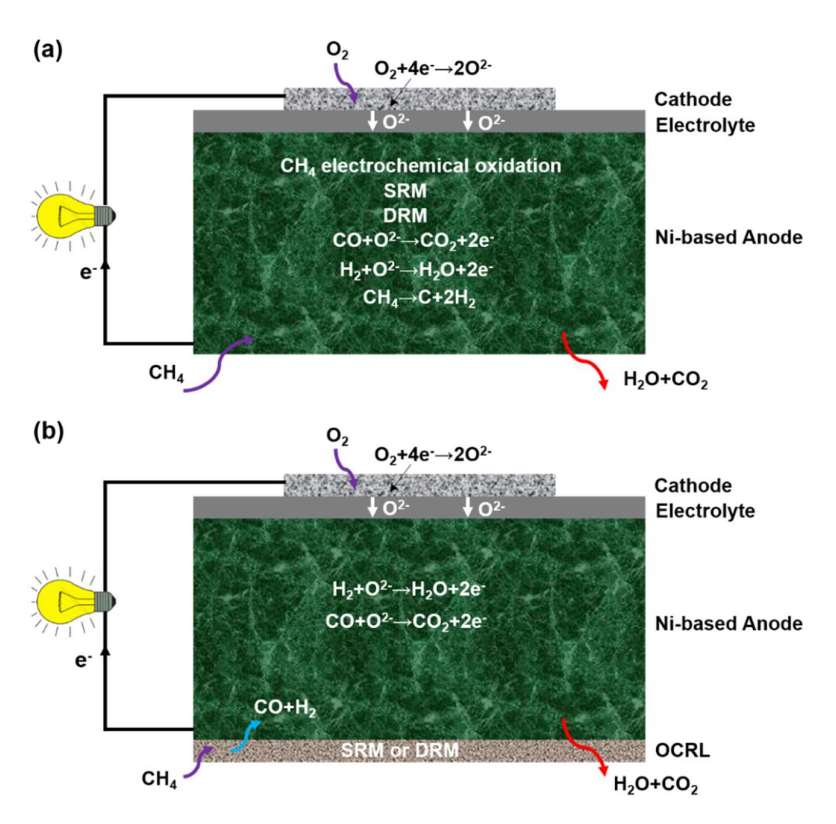


Figure 4 Schematic diagrams of methane conversion in Ni-based anode with (a) and

without (b) OCRL above 600 °C.

## 3. OCRL materials

There have been extensive studies on the reforming catalyst materials, which mainly focus on the catalytic activity, coking resistance and sintering resistance. Apart from the reforming activity of methane and good resistance against carbon growth, OCRL also requires matched thermal expansion coefficient (TEC) and chemical compatibility with the Ni-based anode due to the direct contact between OCRL and the Ni-based anode. The reforming catalytic materials are typically consisted of active component, substrate and catalytic promoter. The catalytic activity, sintering resistance and coking resistance of methane reforming catalysts mainly depend on the type and particle size of active component, the property and specific surface area of substrate, the interaction between the active component and the substrate, etc. [63, 64]. Although some remarkable goals have been achieved in the researches on OCRL materials in terms of reforming activity, mechanical and chemical compatibility with Ni-based anode and coking resistance, there are still many challenges remaining. This review summarizes the influence of each composition on the properties of the OCRL materials and some common OCRL materials, and intending to provide enlightenment and direction for further development of OCRL materials.

## 3.1 Active component of OCRL materials

The active component of OCRL materials is typically metal catalysts for reforming reactions. Due to the endothermic nature of methane reforming reactions, including DRM and SRM, carbon deposition and sintering of the catalyst are inevitable at SOFC operating temperature which is typically higher than 750 °C. To maintain the high efficiency of SOFC, such high operating temperature is required. Therefore, thermal stability is of great importance for the catalyst of OCRL material to avoid deactivation caused by carbon deposition and sintering. So far, the most investigated catalysts for methane reforming are categorized by noble metals and non-noble VIII group metals [65, 66].

Noble metals such as Rh, Ru, Ir, Pd, Pt typically have excellent catalytic activity for

reforming as well as superior coking resistance, which has been demonstrated by many reports [67-72]. The superior ability of these catalysts to eliminate coking can be attributed to their high dispersion and small particle size on the substrates. Among these noble metal catalysts, Rh supported catalyst exhibits the highest catalytic activity and thermal stability, followed by Ru, Ir, Pd and Pt [61]. Pd and Pt supported catalysts show relatively lower thermal stability because of the sintering of these particles at increasing operating temperature [73, 74]. In order to achieve high catalytic activity, thermal stability and coking resistance, it is critical for noble metal catalysts to maintain high dispersion, large surface area and small particle size during operation [75-78]. The first OCRL material adopted on Ni-based anode of SOFC is Ru-CeO<sub>2</sub>, which is first proposed by Zhan et al. [79]. By adding Ru-CeO<sub>2</sub> OCRL on the anode of SOFC, direct internal reforming toward isooctane could be achieved, with high peak power density (PPD) values of 300~600 mW cm<sup>-2</sup> at 670~770 °C. These results greatly promoted the development of direct hydrocarbon SOFCs. However, the bond between Ru-CeO<sub>2</sub> OCRL and Ni-based ceramic anode could be destroyed after multiple thermal cycles. Wang et al. [80] synthesized Ru-Al<sub>2</sub>O<sub>3</sub> by glycine-nitrate combustion method, and used it as a catalyst layer for a SOFC operating on methane fuel. In consideration of catalytic activity, cost and operational stability, the most suitable Ru loading was 3 wt.%. Moreover, the strong interaction between RuO<sub>x</sub> with the Al<sub>2</sub>O<sub>3</sub> supported of 3 wt.% Ru-Al<sub>2</sub>O<sub>3</sub> catalyst was evidenced by H<sub>2</sub>-TPR and TEM, as shown in Figure 5a and 5b. The 3 wt.% Ru-Al<sub>2</sub>O<sub>3</sub> catalyst was exploited as an OCRL in a Ni-Zr<sub>0.92</sub>Y<sub>0.08</sub>O<sub>2-δ</sub> (YSZ) anode support single cell. After several thermal cycling and redox cycling tests, firm adhesion of 3 wt.% Ru-Al<sub>2</sub>O<sub>3</sub> OCRL on the anode surface was presented, as shown in Figure 5c and 5d, suggesting excellent mechanical compatibility between OCRL with Ni-YSZ anode during operation. When fed with CH<sub>4</sub>-CO<sub>2</sub> and CH<sub>4</sub>-H<sub>2</sub>O, the single cell with OCRL reached high PPD, as shown in Figure 5e and 5f, suggesting excellent SRM and DRM catalytic activities of 3 wt.% Ru-Al<sub>2</sub>O<sub>3</sub> OCRL. Outstanding stability was also shown for the single cell with 3 wt.% Ru-Al<sub>2</sub>O<sub>3</sub> OCRL, as only slight drop of ~3.6% in voltage was observed after operation period of 400 min when fed with pure methane

under a current density of 600 mA cm<sup>-2</sup> at 750 °C. Such enhanced stability was attributed to the excellent coking resistance and high reforming efficiency of 3 wt.% Ru-Al<sub>2</sub>O<sub>3</sub> OCRL.

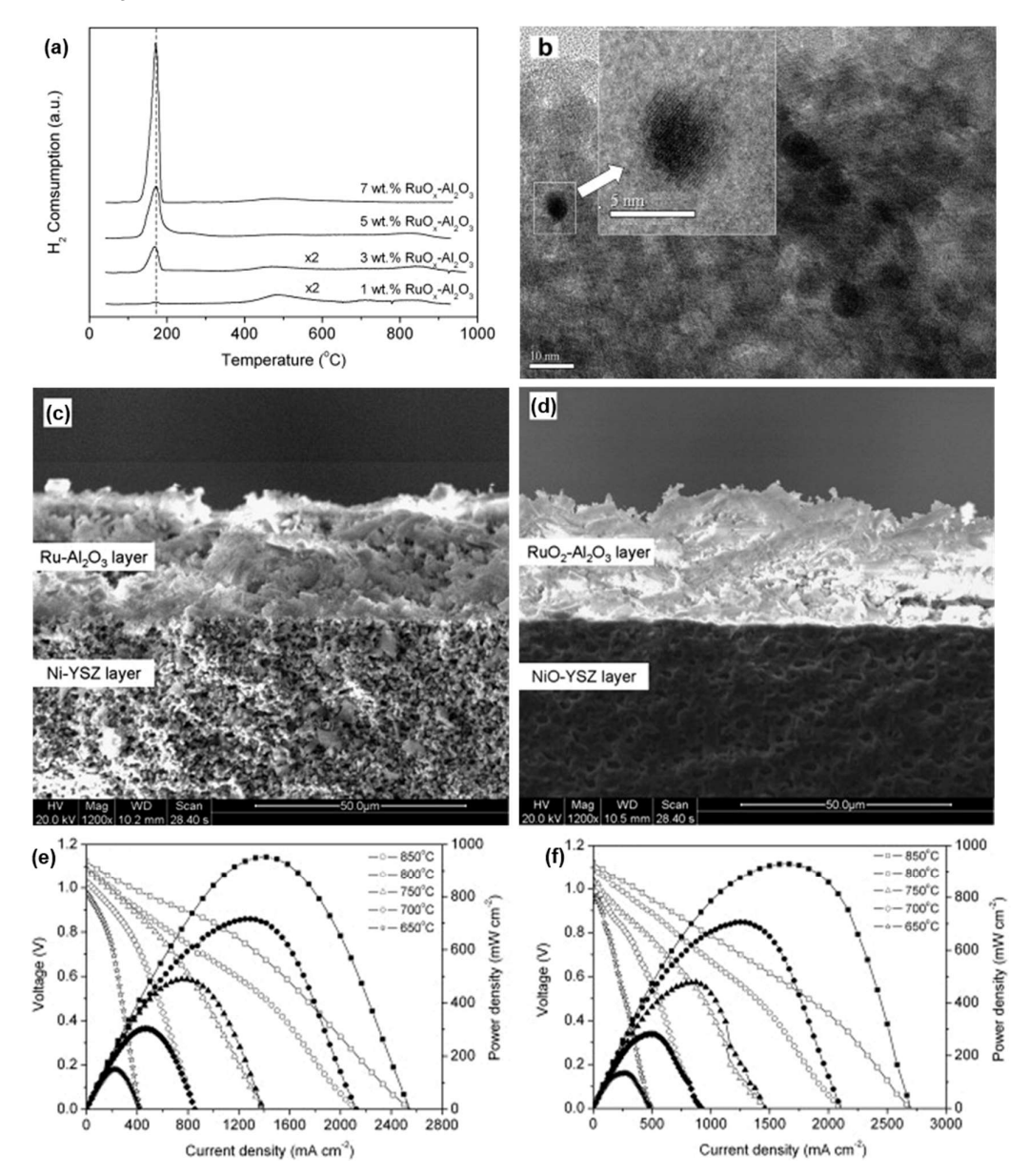


**Figure 5** (a) H<sub>2</sub>-TPD profiles of 7 wt.%, 5 wt.%, 3 wt.% and 1 wt.% RuO<sub>x</sub>-Al<sub>2</sub>O<sub>3</sub> catalysts; (b) TEM image of 3 wt.% Ru-Al<sub>2</sub>O<sub>3</sub> catalyst after reduction; (c) SEM image of the cell with 3 wt.% Ru-Al<sub>2</sub>O<sub>3</sub> OCRL after the redox cycling; (d) SEM image of the cell with 3 wt.% Ru-Al<sub>2</sub>O<sub>3</sub> OCRL after the thermal cycling; (e) *I-V-P* curves of the single cell with 3 wt.% Ru-Al<sub>2</sub>O<sub>3</sub> OCRL when fed with CH<sub>4</sub>-H<sub>2</sub>O (2:1); (f) *I-V-P* curves of the single cell with 3 wt.% Ru-Al<sub>2</sub>O<sub>3</sub> OCRL when fed with CH<sub>4</sub>-CO<sub>2</sub> (2:1) [80].

Although noble metal catalysts exhibit excellent reforming catalytic performance with promising coking resistance and noticeable thermal stability, the practical utilization of these catalysts are severely hindered by their high cost and limited availability. Thus, non-noble supported metal catalysts, typically VIII group transition metals such as Ni, Fe and Co, have attracted increasing attention because of their low cost, high availability and catalytic activity recently. However, serious carbon deposition on non-noble metal catalysts still limits their wide application in methane reforming. It has been reported that the carbon deposition on Ni and Co catalysts are considerably high at 24 mg coke/g cat h and 49.4 mg coke/g cat h, respectively [61]. For non-noble metal catalysts, maintaining high dispersion, surface area and small particle size can effectively extend the catalyst's activation time [77, 81]. In order to solve the coking issue of Ni-YSZ anode when fed with biogas (mainly containing methane and CO<sub>2</sub>), Lyu et al. [82] modified the Ni-YSZ anode by introducing a Ni-Ce<sub>0.9</sub>Gd<sub>0.1</sub>O<sub>2-\delta</sub> (GDC) OCRL via mechanical mixing method. The single cell modified by Ni-GDC OCRL had a PPD of 271 mW cm<sup>-2</sup> at 600 mA cm<sup>-2</sup> when fed with CH<sub>4</sub>/CO<sub>2</sub>, about 3.3 time higher than the PPD achieved by the bare cell. Although the ohmic resistance  $(R_0)$  of the cell slightly increased, the polarization resistance  $(R_p)$  decreased significantly under CH<sub>4</sub>/CO<sub>2</sub>, leading to the decrease of overall resistance and significantly enhanced reforming reaction by the additional OCRL. The introduction of Ni-GDC OCRL also improved the stability of the single cell when fed with CH<sub>4</sub>/CO<sub>2</sub>, which was verified under the operating current densities of 100, 200 and 260 mA cm<sup>-2</sup>. However, serious carbon deposition was detected in the OCRL when the test time exceeded 50 h and more efforts were needed to improve the coking resistance of Ni-GDC OCRL. Large metal particle size and small surface area of the substrate, which derived from the backward preparation process, are the main reasons for coking of Ni-GDC OCRL. Zhao et al. [83] developed NiO-La<sub>2</sub>Ce<sub>2</sub>O<sub>7</sub> (LDC) and NiO-La<sub>1.95</sub>Sm<sub>0.05</sub>Ce<sub>2</sub>O<sub>7</sub> (LSDC) OCRLs by a sol-gel method in Ni-Ce<sub>0.8</sub>Sm<sub>0.2</sub>O<sub>2-δ</sub> (SDC) anode supported SOFC. After in-situ reduction at 650 °C, Ni was homogeneously distributed on the surface of fluorite-type LDC/LSDC substrate. This surface

configuration was beneficial for methane reforming and coking resistance because of the superior water adsorption capacity of LDC/LSDC, which alleviates carbon deposition and achieves excellent catalytic activity of Ni for MSR. In addition, the high stability of LDC/LSDC under H<sub>2</sub>O/CO<sub>2</sub> atmosphere also guarantees it as a promising catalyst substrate. As shown in Figure 6, when fed with wet methane, PPD of bare cell and the cells with Ni-LDC and Ni-LSDC OCRL were 580, 699 and 639 mW cm<sup>-2</sup>, respectively, suggesting enhanced electrochemical performance of the cells with OCRL. In addition, the cells with Ni-LDC and Ni-LSDC OCRL showed relatively better stability for 26 h in wet methane at 0.2 A cm<sup>-2</sup> and 650 °C with no visible carbon deposition in OCRL, while the bare cell failed in just 10 h. The addition of Ni-LDC and Ni-LSDC OCRL improved the electrochemical performance and stability of Ni-SDC anode supported SOFC significantly, and the possible mechanism was proposed as following. Taking Ni-LDC OCRL as an example, the steam from wet methane and from the exhaust gas (containing steam and CO<sub>2</sub>) generated on the anode was absorbed onto LDC due to its ultra-high water adsorption capability and sufficient oxygen vacancies. With Ni as catalyst, the fed methane could undergo SRM and DRM using absorbed water and CO<sub>2</sub> on LDC, transforming into syngas before entering Ni-SDC anode. Since Ni-based anode has higher electrochemical activity and better coking resistance against syngas than methane [84], the electrochemical performance and stability of cell with LDC OCRL were enhanced compared to bare cell when fed with wet methane.

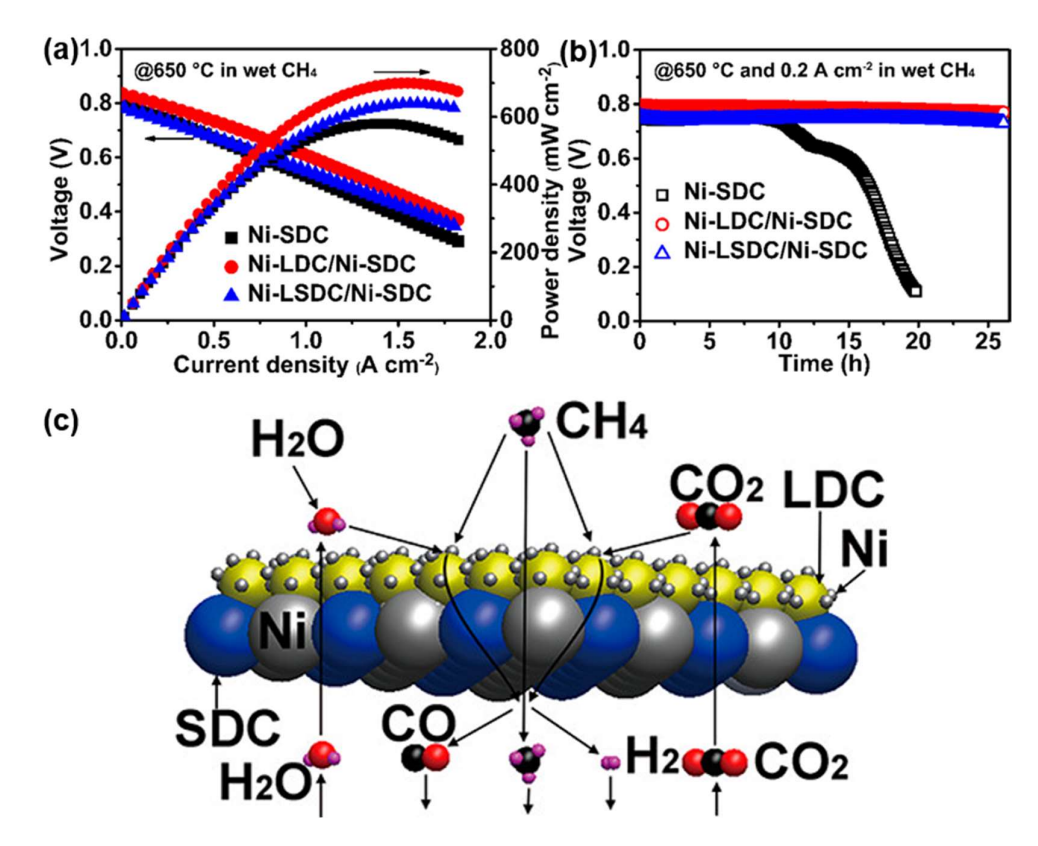


**Figure 6** *I-V-P* curves (a) and stability (b) of the bare cell and the cell with Ni-LDC and Ni-LSDC OCRL when fed with wet methane; (c) Proposed schematic diagram of the cell with Ni-LDC OCRL [83].

Despite these mono-metallic catalysts, the addition of noble metals such as Rh, Pt, Pd or Ru to Ni-based catalysts can improve the reforming catalytic activity and coking resistance of Ni-based catalysts [85-89]. The presence of noble metals keeps Ni in the form of an active metal, thereby minimizing the formation of Ni oxides, resulting in almost no loss of catalytic activity [86, 90]. Alemany *et al.* [86] loaded Ni and Rh-Ni nano-catalysts on nanofiber alumina for the production of syngas through DRM and SRM, and the influence of Rh addition on Ni-Al<sub>2</sub>O<sub>3</sub> catalyst was analyzed. The results showed that the introduction of Rh could improve the reducibility and stability of Ni particles, avoid Ni aggregation and inhibit coking, even at a low Rh loading (in an atomic ratio of 1: 100).

Recently, a new approach for improving the reforming catalytic performance has been reported using bi-metallic catalysts. In addition to higher catalytic activity, bimetallic catalysts also have better coking resistance than mono-metallic-based catalysts. The depletion of carbon deposition can be attributed to the interaction between the doped metal with other metal. Furthermore, the "dopant-like" effect from the doped metal combined with the role of the support affects total reforming catalytic activity of the catalyst [91]. Despite of the relatively low catalytic activity of Fe, Co, Cu when used in mono-metallic catalysts [92], they can potentially play vital roles in bimetallic catalysts. Compared with pure Ni-based catalyst, Fe-M (M= Fe, Co, Cu) catalysts possess higher catalytic activity toward reforming [93]. Co is the most suitable metal to modify Ni-based catalysts because the electronic interaction between Ni and Co helps disperse the metal alloy and inhibits carbon deposition [93]. In addition, the strong Co-O interaction helps the adsorption of CO<sub>2</sub>, and the addition of Co helps prevent carbon deposition on the catalyst [92, 94-96]. The addition of Cu promotes the catalytic activity and sintering resistance due to the strong metal-support interactions and high dispersion of Cu nanoparticles [97]. In a study by Hua et al. [98], an OCRL consisting of a Ni<sub>0.8</sub>Co<sub>0.2</sub>-La<sub>0.2</sub>Ce<sub>0.8</sub>O<sub>1.9</sub> (NiCo-LDC) composite was incorporated into the anode support of H-SOFC. The multiple-twinned bimetallic nanoparticles were proven to have superior activity towards DRM without coking, which can be attributed to the alloying Ni with Co, the strong metal-support interaction as well as the enhanced oxygen storage capacity and accelerated CO<sub>2</sub> absorption on LDC support. In comparison to the conventional design, this layered H-SOFC demonstrated drastically improved CO<sub>2</sub> resistance and DRM efficiency. When fed with CH<sub>4</sub>-CO<sub>2</sub>, the PPD exceeded 910 mW cm<sup>-2</sup> at 700 °C, and could be operated continuously and stably for more than 100 h under the current density of 1 A cm<sup>-2</sup>. Since the reforming catalytic activity of Cu-based catalyst is low, the addition of a second phase catalyst is needed to improve fuel utilization when fed with hydrocarbon. Jin et al. [99] synthesized a Cu<sub>1.3</sub>Mn<sub>1.7</sub>O<sub>4</sub> spinel oxide and characterized it as an anode internal reforming layer for Ni-SDC anode support SOFC directly operating on methane. After *in-situ* reduction by methane, a highly dispersed nano-Cu metal network in the matrix of MnO was obtained. When fed with methane, PPDs of 242 and 311 mW cm<sup>-2</sup> at 650 and 700 °C were

achieved in the fuel cells with Cu<sub>1.3</sub>Mn<sub>1.7</sub>O<sub>4</sub> OCRL, showing ~ 30% improvement in the cell power output compared with cells without OCRL under the same operating conditions. More importantly, the stability of cell performance was also greatly improved with Cu<sub>1.3</sub>Mn<sub>1.7</sub>O<sub>4</sub> OCRL due to the stability of MnO and the strong interaction between MnO and Cu which delivers excellent catalyst durability. In another investigation by Ye *et al.* [100], the addition of a Cu-CeO<sub>2</sub> catalyst layer to the supported anode surface also improved the electrochemical performance and durability of the cell without coking. However, some problems still limit the widespread use of Cu-based catalysts. For example, the melting point of Cu is only 1083 °C, which makes the thermal stability of Cu-based catalysts poor. Moreover, even if the second phase catalyst is added, the catalytic activity of the Cu-based catalyst is still limited. Some other examples about the multi-metallic-based catalysts are shown in **Table 1**.

Apart from the material type of active component, the particle size of the active component plays an important role in the coking resistance of the methane reforming catalysts. According to a study by Zhan *et al.* [101], coking is proportional to Ni particle size, but this trend ceases when Ni particle size is below 6.2 nm. A critical Ni size of no more than 6 nm is required to inhibit coking effectively. Therefore, the particle size of the active component is key to coking resistance.

#### 3.2 Substrate of OCRL materials

The catalytic performance of transition metal catalyst not only depends on the active component itself, but also on the support material for catalyst, especially for Ni-based catalysts [65, 102]. The substrate of reforming catalyst can either be the dispersant, binder or support for the active component. The substrate itself may not have reforming catalytic activity, however, its structure and properties are essential for the reforming catalytic activity, sintering resistance and coking resistance [103]. The requirement for the substrate of OCRL materials are mainly focus on the micro-structure and chemical properties, such as porosity, specific surface area, thermal stability, redox characteristics, etc. Substrates with high porosities and large specific surface areas can improve the dispersion of the metal catalyst, leading to better sintering resistance, and

facilitating the reactants adsorption in the reaction [103]. Moreover, the interaction between the active component and the substrate material affects the stability and reducibility of the catalysts [104]. The redox ability of the support itself can improve the catalytic activity of the reforming catalyst. For methane reforming catalysts, the adsorption performance of the substrate materials for CO<sub>2</sub>/H<sub>2</sub>O plays a significant role in the catalytic activity and coking resistance of the catalysts. In addition, as the OCRL of the single cell, the catalyst substrate materials must have matched TEC and good chemical compatibility with the SOFC anode because of the direct contact between the catalyst and the Ni-based anode. Additionally, when selecting the substrate materials, the stability under high temperature CO<sub>2</sub>/H<sub>2</sub>O atmosphere should also be considered.

During the research and development of reforming catalysts, some perovskite oxides (ABO<sub>3</sub>) composed of rare earth metal elements at the A-site and transition metal elements at the B-site are found to have the advantages of sufficient oxygen vacancies and high thermal stability. As the substrate of reforming catalyst, the lattice defects (e.g. oxygen vacancies) in the perovskite oxides can promote the surface oxygen adsorption performance and enhance the migration ability of lattice oxygen [105]. Recently, perovskite oxides have been reported a wide range of applications in methane reforming reactions. Some perovskite oxides can be completely decomposed in a reducing atmosphere, and the decomposition products contain substrate and active component, which can be used as OCRL materials. Wei et al. [106] synthesized Ni-doped LaMnO<sub>3</sub>δ (La<sub>0.9</sub>Mn<sub>0.8</sub>Ni<sub>0.2</sub>O<sub>3-δ</sub>, LMN) by a sol-gel method and used it for DRM. After reduction in 5%H<sub>2</sub>-N<sub>2</sub>, in-situ exsolved Ni nanoparticles were evenly distributed on the surface of the substrate, and the substrate could still maintain the perovskite structure. TEM was conducted to analyze the reduced LMN (R-LMN). It was found that the exsolved Ni nanoparticles were partially embedded in the substrate, as shown in **Figure 7a** and 7b, and there was a strong interaction between Ni nanoparticles and substrate. After performing 24-hours of DRM reaction at 700 °C, no obvious carbon deposition could be observed. Ni nanoparticles still maintained the highly dispersed condition with no obvious sintering as shown in Figure 7c.

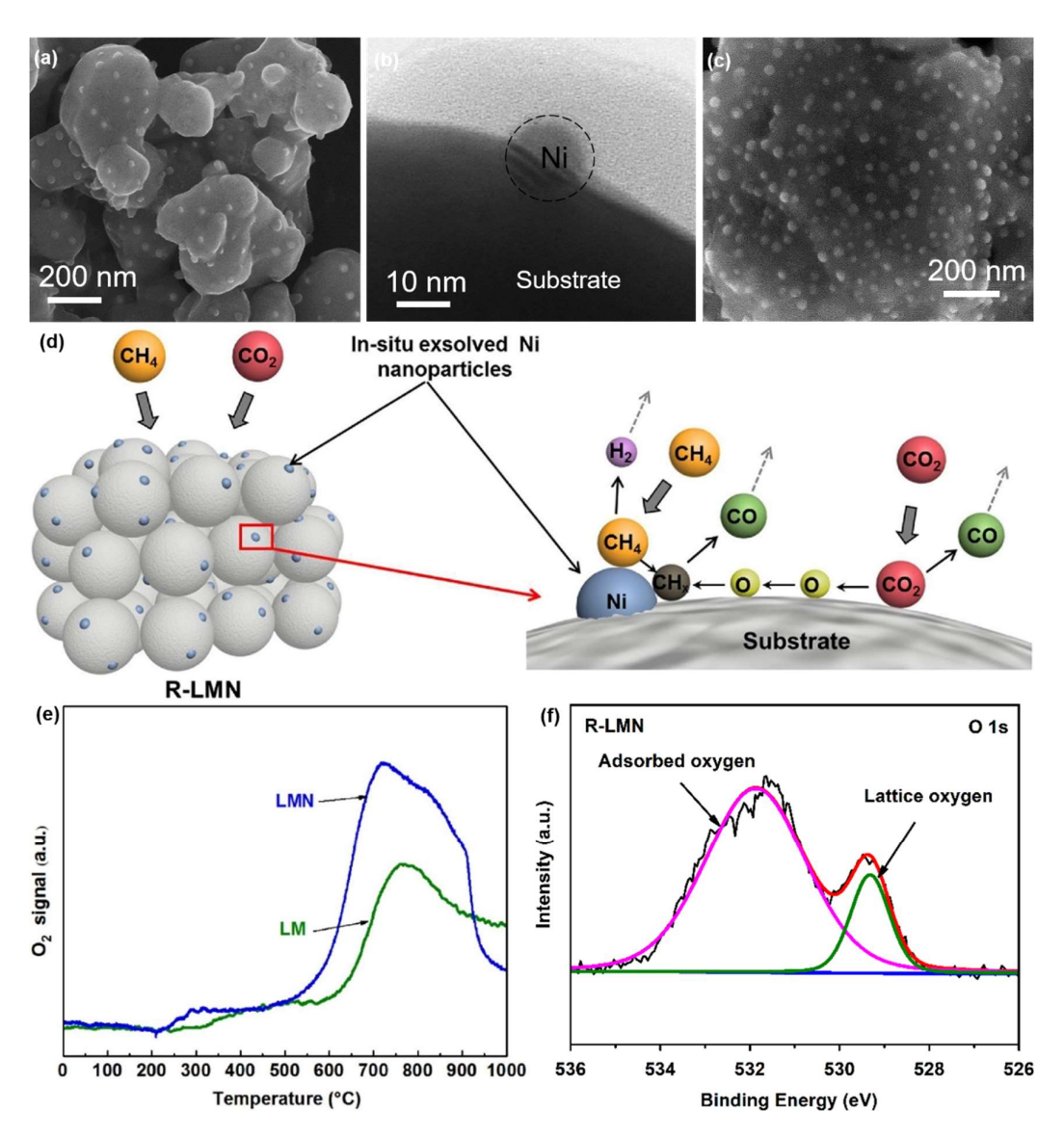


**Figure 7** (a) SEM image of R-LMN; (b) TEM image showing partial embedment of the exsolved Ni nanoparticle into the substrate; (c) Microstructure of R-LMN after 24-hours DRM test; (d) Schematic mechanism for DRM; (e) O<sub>2</sub>-TPD profiles of LMN and LM; (f) O-XPS spectra pf R-LMN [106].

Some oxides such as CeO<sub>2</sub>, La<sub>2</sub>O<sub>3</sub>, ZrO<sub>2</sub> and Al<sub>2</sub>O<sub>3</sub> have a strong ability to adsorb H<sub>2</sub>O/CO<sub>2</sub> and are often used as support for methane reforming catalysts [84, 107-112]. Wan *et al.* [112] introduced a Ni-La<sub>2</sub>O<sub>3</sub> OCRL over a traditional Ni-BaZr<sub>0.4</sub>Ce<sub>0.4</sub>Y<sub>0.2</sub>O<sub>3-δ</sub> (Ni-BZCY) anode for DRM through the *in-situ* reduction of La<sub>2</sub>NiO<sub>4</sub> (LN). After complete reduction in H<sub>2</sub> at 700 °C for 2 h, the Ni particles were highly dispersed and uniformly distributed on the surface of La<sub>2</sub>O<sub>3</sub>. At 700 °C, the reduced LN (R-LN)

showed much higher CO<sub>2</sub> conversion and CO selectivity than bare Ni-BZCY anode, as shown in Figure 8a, indicating good DRM catalytic activity of R-LN. Moreover, after exposing R-LN to CH<sub>4</sub>-CO<sub>2</sub> atmosphere, Ni and a new phase of La<sub>2</sub>O<sub>2</sub>CO<sub>3</sub> were detected, which was considered to be an intermediate product of great importance in the DRM and attributed to the coking resistance [113-118]. The formation of La<sub>2</sub>O<sub>2</sub>CO<sub>3</sub> indicates that CO<sub>2</sub> is adsorbed on La<sub>2</sub>O<sub>3</sub> during DRM, which helps to maintain the insufficient stability of BZCY in CH<sub>4</sub>-CO<sub>2</sub> atmosphere. Meanwhile, the small size of Ni particles and its high dispersion could also be beneficial for coking resistance and sintering resistance. When fed with pure H<sub>2</sub>, there was not much difference between the PPD values of bare H-SOFC and layered H-SOFC, as shown in **Figure 8b**. However, when fed with CH<sub>4</sub>-CO<sub>2</sub>, layered H-SOFC showed a higher PPD value, 120 mW cm<sup>-2</sup>, than that of the bare H-SOFC at 700 °C (~90 mW cm<sup>-2</sup>), as shown in Figure 8c, suggesting excellent DRM catalytic activity of R-LN OCRL. The operation stability of both cells when fed with CH<sub>4</sub>-CO<sub>2</sub> was also examined, as shown in Figure 8d. The voltage of layered H-SOFC had no obvious change under a polarization current density of 200 mA cm<sup>-2</sup> for 350 min and no carbon deposition could be detected, suggesting that H-SOFC can work stably in CH<sub>4</sub>-CO<sub>2</sub> fuel after the introduction of R-LN OCRL. While for bare H-SOFC, the voltage kept decreasing during the test even under a smaller polarization current density of 133 mA cm<sup>-2</sup>.

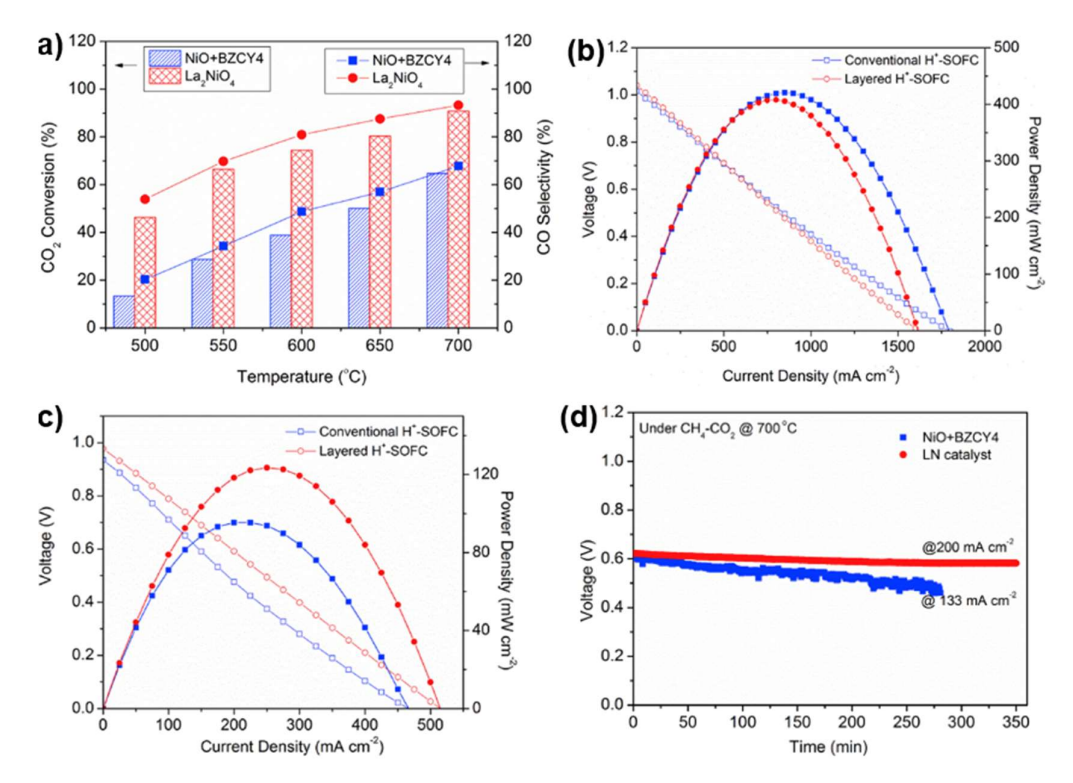


**Figure 8** (a) Conversion of CO<sub>2</sub> and selectivity of CO over the Ni-BZCY anode and R-LN catalyst during DRM at various operating temperatures; (b) *I-V-P* curves of bare H-SOFC and layered H-SOFC at 700 °C when fed with H<sub>2</sub>; (c) *I-V-P* curves of bare H-SOFC and layered H-SOFC at 700 °C when fed with CH<sub>4</sub>-CO<sub>2</sub>; (d) Time dependence of the voltage under a proper constant polarization current density at 700 °C [112].

Commonly used electrolyte materials such as BaZr<sub>0.1</sub>Ce<sub>0.7</sub>Y<sub>0.1</sub>Yb<sub>0.1</sub>O<sub>3-δ</sub> (BZCYYb), GDC, SDC, etc. are usually selected as the catalyst substrate because of their excellent CO<sub>2</sub>/H<sub>2</sub>O adsorption capacity, which is beneficial to the elimination of coking [45, 82, 119, 120]. Moreover, the matched TEC and good chemical compatibility with Ni-based anode ensure good connectivity between OCRL and Ni-based anode. In a study from Hua *et al.* [121], a Ni-Cu-Fe alloy-BZCYYb OCRL on the surface of the Ni-YSZ anode supported cell was prepared and investigated in dry and wet (3 mol% H<sub>2</sub>O) methane. Compared to the conventional anode supported cell, the durability of the cell with OCRL was significantly improved when fed with dry methane. Insignificant coking occurred in the anode of the cell with OCRL when exposed to dry methane at 200 mA cm<sup>-2</sup>. However, the addition of H<sub>2</sub>O at a low content as 3 mol% can remove the formed

carbon attributable to the presence of BZCYYb which is prone to H<sub>2</sub>O adsorption.

# 3.3 Catalytic promoter and preparation method for OCRL

Catalytic promoters are auxiliary components of the catalyst. Despite of no catalytic activity or low catalytic activity of catalytic promoters, they can improve the catalytic activity, selectivity and stability of the catalysts after the addition [122, 123]. For methane reforming catalysts, the addition of catalytic promoters can change the acidity or basicity of the catalyst surface, improve the dispersion of active components, enhance the interaction between the active components and the substrate, and change the electron density distribution of the active component metals [124], thereby improving the catalytic activity, sintering resistance and coking resistance of the catalysts. For methane reforming catalysts, acidic substrate can easily lead to coking. Using alkaline catalytic promoter to reduce the acidity of the catalyst surface is an effective way to alleviate coking. For methane reforming catalysts, the commonly used catalytic promoters are rare earth metal oxides such as CeO<sub>2</sub> [125], and alkaline earth metal oxides such as CaO and MgO [126].

The preparation process of the methane reforming catalyst also has a great influence on the acidity and basicity of the substrate, the particle size and dispersion of the active component, and the interaction between the active component and the substrate, which in turn affects the catalytic activity, sintering resistance and coking resistance of the methane reforming catalyst. The common preparation methods of methane reforming catalysts are sol-gel, mechanical mixing, solution infiltration, co-precipitation, etc. [82, 127, 128]. Among them, solution infiltration is the most commonly used method for preparing supported catalysts [129]. However, the poor reproducibility, the uneven distribution of active components on the surface of substrate, and the weak interaction between the active components and the substrate make the solution infiltration method very challenging for practical implementation.

Nowadays, sol-gel-*in situ* exsolution method has received more and more attention [106, 130, 131]. The active component metal elements are firstly doped into the crystal lattice of the catalyst precursor. After high-temperature calcination and high-

temperature reduction, a highly dispersed and stable nano-sized active components are finally exsolved on the surface of the parent oxide. The active components are embedded inside the substrate with a strong interaction, which is beneficial to coking resistance and coarsening of the methane reforming catalysts.

## 3.4 Reforming mechanism

Whether it is a noble metal or non-noble metal catalyst, there is a consensus regarding to the mechanism of methane reforming reaction: methane is activated on the metal and CO<sub>2</sub> or H<sub>2</sub>O is activated on the supports [132, 133]. With the catalysis of active component, H atoms in methane are released one by one, and finally the activated carbon remains on the surface of the metal particles. CO2 (or H2O) adsorbs and dissociates into CO (or H<sub>2</sub>) and oxygen atoms on the surface of substrate. Oxygen atoms then enter the lattice of the substrate and are transferred to the active component/substrate interface to oxidize the activated carbon. The activation time of the catalyst depends on the rate of carbon removal and formation [134]. Activated carbon forms at the active component/substrate interface, and grows in the form of carbon nanofibers or nanotubes [27, 135, 136]. The metal particles (active component) are then uplifted, causing the deactivation of the catalyst. With increasing the metal particle size and decreasing bond strength with the substrate, more carbon dissolution could occur into the metal particles and the particles are easier to be uplifted from the substrate, leading to quicker carbon deposition [137, 138]. When the metal particles are small enough and partially embedded into the substrate through a strong interfacial bond, only limited amount of carbon can be dissolved into the metal particles, and the formation of carbon at the active component/substrate interface is prevented. In this case, activated carbon can only remain on the surface of metal particles and may be further oxidized by oxygen atoms. Obviously, the dissociation and adsorption capacity of the substrate for CO<sub>2</sub> (or H<sub>2</sub>O) as well as the oxygen transport capability are critical properties to the material's reforming catalytic activity and resistance to carbon deposition.

In Wei's study [106], the process of DRM and coking resistance phenomenon of R-

LMN catalyst have been analyzed and summarized, as shown in **Figure 7d**. Methane is decomposed into C groups and H<sub>2</sub> on Ni nanoparticles, and the steps are as follows.

$$CH_4 + L_1 \to L_1 * CH_4 \tag{11}$$

$$L_1 * CH_4 + L_1 \rightarrow L_1 * CH_3 + H * L_1$$
 (12)

$$L_1 * CH_3 + L_1 \to L_1 * CH_2 + H * L_1$$
 (13)

$$L_1 * CH_2 + L_1 \rightarrow L_1 * C + 2H * L_1$$
 (14)

$$2H * L_1 \to H_2 + 2L_1 \tag{15}$$

On an alkaline substrate, CO<sub>2</sub> is activated and dissociated into CO, the steps are as follows.

$$CO_2 + L_2 \rightarrow L_2 * CO_2 \tag{16}$$

$$L_2 * CO_2 \rightarrow CO + L_2 * O \tag{17}$$

$$L_2 * O + L_1 * C \rightarrow L_1 + L_2 + CO$$
 (18)

 $L_1$  is the active site on Ni nanoparticles, and  $L_2$  is the active site on the substrate. According to the above steps, the adsorption and dissociation of CH<sub>4</sub> on Ni nanoparticles and the adsorption and dissociation of CO<sub>2</sub> on the perovskite oxide substrate are the rate-controlling steps of DRM.

The authors believed that the exsolved Ni nanoparticles were partially embedded in and maintained a strong interaction with the perovskite oxide substrate, which prevented the formation of carbon nanofibers or carbon nanotubes. XPS and oxygen adsorption and desorption characterizations, as shown in **Figure 7e** and **7f**, suggested that LMN had more oxygen vacancies than lanthanum manganate (La<sub>0.9</sub>MnO<sub>3-δ</sub>, LM), which can conduct more lattice oxygen to the surface and is conducive to the adsorption and dissociation of CO<sub>2</sub> as well as the rapid elimination of deposited carbon. In summary, the authors speculated a preliminary reforming reaction and coking resistance mechanism for the R-LMN. Ni nanoparticles provided abundant active sites for the activation and cracking of methane while preventing the formation of carbon nanofibers; the perovskite oxide substrate provided sufficient oxygen species for the adsorption and dissociation of CO<sub>2</sub>, which could quickly oxidize the C groups formed on the surface of Ni particles to ensure the elimination of deposited carbon. In addition to excellent

reforming catalytic performance and coking resistance, LMN has good chemical compatibility and matched TEC with common Ni-based anodes. These advantages make LMN the potential an OCRL material.

# 4. Conclusions, challenges and prospects

Efficient utilization of methane, which is the most important hydrocarbon fuel, in SOFCs is of great significance to the commercialization and broad application of SOFCs. Direct utilization of methane, however, will cause severe carbon deposition in the anode and rapid degradation of cell performance for the conventional Ni-based anode supported SOFCs. Fuel reforming technologies, including steam reforming and dry reforming, are common methods are developed to utilize methane in SOFCs. Reforming methane into syngas, which can be more easily electrochemically oxidized by SOFCs, can greatly improve cell performance and reduce carbon deposition. OCRL is a typical internal reforming design, which can reform methane into syngas before entering the anode of SOFCs. Its on-cell design can simplify the system, reduce cost and improve energy efficiency of SOFCs. Moreover, the material selection is more flexible without being restricted by anode materials.

Excellent catalytic activity for the reforming reaction of methane, good coking resistance, and matched TEC as well as chemical compatibility with Ni-based anode are the basic requirements for OCRL materials. The reforming catalytic materials are typically consisted of active component, substrate and catalytic promoter. The catalytic activity, sintering resistance and coking resistance of methane reforming catalysts mainly depend on the type and particle size of active component, the property and specific surface area of the substrate, and the interaction between the active component and the substrate. Regardless of the type of reforming catalyst, the mechanism of the methane reforming reaction seems to be identical: methane is activated on the metal, while CO<sub>2</sub> or H<sub>2</sub>O is activated on the support. The catalytic activity of the catalyst for methane reforming and carbon deposition depends on the type of metal used, the nature of the support, the surface area of the support, the particle size of the metal, and the interaction between the metal and the support.

There have been many relevant studies on the application of OCRL in direct methane SOFCs. Improved electrochemical performance and durability are shown after the introduction of OCRL. Nevertheless, some issues still limit the widespread application of OCRL design. The OCRL has a certain hindrance to the mass transfer process of fuel gas. Therefore, how to control its porosity and microstructure is an urgent problem to be solved. Compared with the Ni-based anodes, insufficient electronic conductivity of OCRL will affect the current collection on the anode side of SOFCs. Moreover, the fuel flow rate needs to be limited in order to avoid carbon deposition as much as possible when using OCRL. Therefore, it is imperative to develop OCRL materials with higher reforming catalytic activity. The development of direct methane SOFCs has a significant role in promoting the commercialization of SOFCs. Therefore, it is of great significance to develop OCRL materials with excellent reforming catalytic activity, high coking resistance and low price.

### Acknowledgements

This research was financially supported by the National Key Research & Development Program of China (2018YFE0124700), the National Natural Science Foundation of China (51872103, 52072134, U1910209) and the U.S. National Science Foundation (DMR-1832809). The help from Project of Shandong Province Higher Educational Young Innovative Talent Introduction and Cultivation Team is gratefully acknowledged.

#### **Declaration of competing interest**

The authors declare that they have no known competing financial interests or personal relationships that could have appeared to influence the work reported in this paper.

#### References

- [1] Zhiznin S, Timokhov V, Gusev A. Economic aspects of nuclear and hydrogen energy in the world and Russia. International Journal of Hydrogen Energy. 2020;45:31353-66.
- [2] Boretti A. Production of hydrogen for export from wind and solar energy, natural gas, and coal in Australia. International Journal of Hydrogen Energy. 2020;45:3899-904.
- [3] He W, Abbas Q, Alharthi M, Mohsin M, Hanif I, Vo XV, et al. Integration of renewable hydrogen in light-duty vehicle: nexus between energy security and low carbon emission resources. International Journal of Hydrogen Energy. 2020;45:27958-68.
- [4] Zhu J, Zhou D, Pu Z, Sun H. A Study of Regional Power Generation Efficiency in China: Based on a Non-Radial Directional Distance Function Model. Sustainability. 2019;11:659.
- [5] Bouman EA, Ramirez A, Hertwich EG. Multiregional environmental comparison of fossil fuel power generation—Assessment of the contribution of fugitive emissions from conventional and unconventional fossil resources. International Journal of Greenhouse Gas Control. 2015;33:1-9.
- [6] Sun S, Awadallah O, Cheng Z. Poisoning of Ni-Based anode for proton conducting SOFC by H<sub>2</sub>S, CO<sub>2</sub>, and H<sub>2</sub>O as fuel contaminants. Journal of Power Sources. 2018;378:255-63.
- [7] Yang X, Chen J, Panthi D, Niu B, Lei L, Yuan Z, et al. Electron doping of Sr<sub>2</sub>FeMoO<sub>6-δ</sub> as high performance anode materials for solid oxide fuel cells. Journal of Materials Chemistry A. 2019;7:733-43.
- [8] Minutillo M, Perna A, Di Trolio P, Di Micco S, Jannelli E. Techno-economics of novel refueling stations based on ammonia-to-hydrogen route and SOFC technology. International Journal of Hydrogen Energy. 2021;46:10059-71.
- [9] Costamagna P, De Giorgi A, Moser G, Pellaco L, Trucco A. Data-driven fault diagnosis in SOFC-based power plants under off-design operating conditions. International Journal of Hydrogen Energy. 2019;44:29002-6.

- [10] Liu J, Barnett SA. Operation of anode-supported solid oxide fuel cells on methane and natural gas. Solid State Ionics. 2003;158:11-6.
- [11] Li M, Hua B, Luo J-L. Alternative Fuel Cell Technologies for Cogenerating Electrical Power and Syngas from Greenhouse Gases. ACS Energy Letters. 2017;2:1789-96.
- [12] Gao Y, Jiang J, Meng Y, Yan F, Aihemaiti A. A review of recent developments in hydrogen production via biogas dry reforming. Energy Conversion and Management. 2018;171:133-55.
- [13] Abdulrasheed A, Jalil AA, Gambo Y, Ibrahim M, Hambali HU, Hamid MYS. A review on catalyst development for dry reforming of methane to syngas: Recent advances. Renewable and Sustainable Energy Reviews. 2019;108:175-93.
- [14] Jang W-J, Shim J-O, Kim H-M, Yoo S-Y, Roh H-S. A review on dry reforming of methane in aspect of catalytic properties. Catalysis Today. 2019;324:15-26.
- [15] Basu RN, Sharma AD, Dutta A, Mukhopadhyay J. Processing of high-performance anode-supported planar solid oxide fuel cell. International Journal of Hydrogen Energy. 2008;33:5748-54.
- [16] Tucker MC. Progress in metal-supported solid oxide fuel cells: A review. Journal of Power Sources. 2010;195:4570-82.
- [17] Zhu W, Deevi S. A review on the status of anode materials for solid oxide fuel cells. Materials Science and Engineering: A. 2003;362:228-39.
- [18] Moon H, Kim SD, Hyun SH, Kim HS. Development of IT-SOFC unit cells with anode-supported thin electrolytes via tape casting and co-firing. International Journal of Hydrogen Energy. 2008;33:1758-68.
- [19] Chan SH. A review of anode materials development in solid oxide fuel cells. Journal of Materials Science. 2004;39:4405-39.
- [20] Jacobson AJ. Materials for Solid Oxide Fuel Cells. Chemistry of Materials. 2010;22:660-74.
- [21] Ge XM, Chan SH, Liu QL, Sun Q. Solid oxide fuel cell anode materials for direct hydrocarbon utilization. Advanced Energy Materials. 2012;2:1156-81.

- [22] Ball M, Wietschel M. The future of hydrogen-opportunities and challenges. International Journal of Hydrogen Energy. 2009;34:615-27.
- [23] Alves HJ, Junior CB, Niklevicz RR, Frigo EP, Frigo MS, Coimbra-Araújo CH. Overview of hydrogen production technologies from biogas and the applications in fuel cells. International Journal of Hydrogen Energy. 2013;38:5215-25.
- [24] Saunders GJ, Preece J, Kendall K. Formulating liquid hydrocarbon fuels for SOFCs. Journal of Power Sources. 2004;131:23-6.
- [25] McPhee WA, Boucher M, Stuart J, Parnas RS, Koslowske M, Tao T, et al. Demonstration of a Liquid-Tin Anode Solid-Oxide Fuel Cell (LTA-SOFC) operating from biodiesel fuel. Energy & fuels. 2009;23:5036-41.
- [26] Wang D, Czernik S, Montane D, Mann M, Chornet E. Biomass to Hydrogen via Fast Pyrolysis and Catalytic Steam Reforming of the Pyrolysis Oil or Its Fractions. Industrial & Engineering Chemistry Research. 1997;36:1507-18.
- [27] McIntosh S, Gorte RJ. Direct Hydrocarbon Solid Oxide Fuel Cells. Chemical Reviews. 2004;104:4845-66.
- [28] Cowin PI, Petit CT, Lan R, Irvine JT, Tao S. Recent progress in the development of anode materials for solid oxide fuel cells. Advanced Energy Materials. 2011;1:314-32.
- [29] Wang W, Su C, Wu Y, Ran R, Shao Z. Progress in Solid Oxide Fuel Cells with Nickel-Based Anodes Operating on Methane and Related Fuels. Chemical Reviews. 2013;113:8104-51.
- [30] Lu X, Zhu J. Cu (Pd)-impregnated La<sub>0.75</sub>Sr<sub>0.25</sub>Cr<sub>0.5</sub>Mn<sub>0.5</sub>O<sub>3-δ</sub> anodes for direct utilization of methane in SOFC. Solid State Ionics. 2007;178:1467-75.
- [31] Yang C, Yang Z, Jin C, Xiao G, Chen F, Han M. Sulfur-tolerant redox-reversible anode material for direct hydrocarbon solid oxide fuel cells. Advanced Materials. 2012;24:1439-43.
- [32] Chen Y, Zhang Y, Xiao G, Yang Z, Han M, Chen F. Sulfur-tolerant hierarchically porous ceramic anode-supported solid-oxide fuel cells with self-precipitated nanocatalyst. ChemElectroChem. 2015;2:672-8.

- [33] Ahmed K, Foger K. Kinetics of internal steam reforming of methane on Ni/YSZ-based anodes for solid oxide fuel cells. Catalysis Today. 2000;63:479-87.
- [34] Takeguchi T, Kani Y, Yano T, Kikuchi R, Eguchi K, Tsujimoto K, et al. Study on steam reforming of CH<sub>4</sub> and C<sub>2</sub> hydrocarbons and carbon deposition on Ni-YSZ cermets. Journal of Power Sources. 2002;112:588-95.
- [35] Horiuchi T, Sakuma K, Fukui T, Kubo Y, Osaki T, Mori T. Suppression of carbon deposition in the CO<sub>2</sub>-reforming of CH<sub>4</sub> by adding basic metal oxides to a Ni/Al<sub>2</sub>O<sub>3</sub> catalyst. Applied Catalysis A: General. 1996;144:111-20.
- [36] Fan MS, Abdullah AZ, Bhatia S. Catalytic technology for carbon dioxide reforming of methane to synthesis gas. ChemCatChem. 2009;1:192-208.
- [37] Murray EP, Tsai T, Barnett SA. A direct-methane fuel cell with a ceria-based anode. Nature. 1999;400:649-51.
- [38] Huang T-J, Huang M-C. Electrochemical promotion of bulk lattice-oxygen extraction for syngas generation over Ni-GDC anodes in direct-methane SOFCs. Chemical Engineering Journal. 2008;135:216-23.
- [39] Babaei A, Li J. Electrocatalytic Promotion of Palladium Nanoparticles on Hydrogen Oxidation on Ni/GDC Anodes of SOFCs via Spillover. Journal of The Electrochemical Society. 2009;156:B1022.
- [40] Nabae Y, Yamanaka I. Alloying effects of Pd and Ni on the catalysis of the oxidation of dry CH<sub>4</sub> in solid oxide fuel cells. Applied Catalysis A: General. 2009;369:119-24.
- [41] Marina OA, Mogensen M. High-temperature conversion of methane on a composite gadolinia-doped ceria-gold electrode. Applied Catalysis A: General. 1999;189:117-26.
- [42] Hibino T, Hashimoto A, Yano M, Suzuki M, Sano M. Ru-catalyzed anode materials for direct hydrocarbon SOFCs. Electrochimica Acta. 2003;48:2531-7.
- [43] Chen G, Guan G, Kasai Y, You H-X, Abudula A. Degradation mechanism of Nibased anode in low concentrations of dry methane. Journal of Power Sources. 2011;196:6022-8.

- [44] Choudhary V, Rane V, Rajput A. Beneficial effects of cobalt addition to Nicatalysts for oxidative conversion of methane to syngas. Applied Catalysis A: General. 1997;162:235-8.
- [45] Li S, Wang S, Nie H, Wen T-l. A direct-methane solid oxide fuel cell with a double-layer anode. Journal of Solid State Electrochemistry. 2007;11:59-64.
- [46] Kan H, Lee H. Enhanced stability of Ni–Fe/GDC solid oxide fuel cell anodes for dry methane fuel. Catalysis Communications. 2010;12:36-9.
- [47] Kee RJ, Zhu H, Goodwin DG. Solid-oxide fuel cells with hydrocarbon fuels. Proceedings of the Combustion Institute. 2005;30:2379-404.
- [48] Chen Y, Zhang Y, Lin Y, Yang Z, Su D, Han M, et al. Direct-methane solid oxide fuel cells with hierarchically porous Ni-based anode deposited with nanocatalyst layer. Nano Energy. 2014;10:1-9.
- [49] Chen Y, Chen F, Wang W, Ding D, Gao J. Sm<sub>0.2</sub>(Ce<sub>1-x</sub>Ti<sub>x</sub>)<sub>0.8</sub>O<sub>1.9</sub> modified Ni–yttria-stabilized zirconia anode for direct methane fuel cell. Journal of Power Sources. 2011;196:4987-91.
- [50] Asamoto M, Miyake S, Sugihara K, Yahiro H. Improvement of Ni/SDC anode by alkaline earth metal oxide addition for direct methane–solid oxide fuel cells. Electrochemistry Communications. 2009;11:1508-11.
- [51] Yang L, Choi Y, Qin W, Chen H, Blinn K, Liu M, et al. Promotion of water-mediated carbon removal by nanostructured barium oxide/nickel interfaces in solid oxide fuel cells. Nature Communications. 2011;2:1-9.
- [52] Murray EP, Barnett SA. Operation of Low-Temperature SOFCs on Pure Methane and Ethane Without Carbon Deposition. SOFC VI Proceedings: Electrochemical Society; 1999.
- [53] Wang JB, Wu Y-S, Huang T-J. Effects of carbon deposition and de-coking treatments on the activation of CH<sub>4</sub> and CO<sub>2</sub> in CO<sub>2</sub> reforming of CH<sub>4</sub> over Ni/yttria-doped ceria catalysts. Applied Catalysis A: General. 2004;272:289-98.
- [54] Horita T, Yamaji K, Kato T, Sakai N, Yokokawa H. Design of metal/oxide interfaces for the direct introduction of hydrocarbons into SOFCs. Journal of Power

- Sources. 2004;131:299-303.
- [55] Gür TM. Comprehensive review of methane conversion in solid oxide fuel cells: prospects for efficient electricity generation from natural gas. Progress in Energy and Combustion Science. 2016;54:1-64.
- [56] Andersson M, Paradis H, Yuan J, Sundén B. Review of catalyst materials and catalytic steam reforming reactions in SOFC anodes. International Journal of Energy Research. 2011;35:1340-50.
- [57] Yang L, Ge X, Wan C, Yu F, Li Y. Progress and perspectives in converting biogas to transportation fuels. Renewable and Sustainable Energy Reviews. 2014;40:1133-52.
- [58] Choudhary V, Uphade B, Mamman A. Simultaneous steam and CO<sub>2</sub> reforming of methane to syngas over NiO/MgO/SA-5205 in presence and absence of oxygen. Applied Catalysis A: General. 1998;168:33-46.
- [59] Brungs AJ, York AP, Claridge JB, Márquez-Alvarez C, Green ML. Dry reforming of methane to synthesis gas over supported molybdenum carbide catalysts. Catalysis Letters. 2000;70:117-22.
- [60] Wang S, Lu G, Millar GJ. Carbon Dioxide Reforming of Methane to Produce Synthesis Gas over Metal-Supported Catalysts: State of the Art. Energy & Fuels. 1996;10:896-904.
- [61] Aramouni NAK, Touma JG, Tarboush BA, Zeaiter J, Ahmad MN. Catalyst design for dry reforming of methane: Analysis review. Renewable and Sustainable Energy Reviews. 2018;82:2570-85.
- [62] Zhu X-Y, Castro M, Akhter S, White J, Houston J. C–H bond cleavage for ethylene and acetylene on Ni (100). Surface Science. 1988;207:1-16.
- [63] Ballarini AD, de Miguel SR, Jablonski EL, Scelza OA, Castro AA. Reforming of CH<sub>4</sub> with CO<sub>2</sub> on Pt-supported catalysts: effect of the support on the catalytic behaviour. Catalysis Today. 2005;107:481-6.
- [64] Avetisov A, Rostrup-Nielsen J, Kuchaev V, Hansen J-HB, Zyskin A, Shapatina E. Steady-state kinetics and mechanism of methane reforming with steam and carbon dioxide over Ni catalyst. Journal of Molecular Catalysis A: Chemical. 2010;315:155-

- [65] Nieva MA, Villaverde MM, Monzón A, Garetto TF, Marchi AJ. Steam-methane reforming at low temperature on nickel-based catalysts. Chemical Engineering Journal. 2014;235:158-66.
- [66] Ligthart D, Van Santen R, Hensen E. Influence of particle size on the activity and stability in steam methane reforming of supported Rh nanoparticles. Journal of Catalysis. 2011;280:206-20.
- [67] Ferreira-Aparicio P, Marquez-Alvarez C, Rodriguez-Ramos I, Schuurman Y, Guerrero-Ruiz A, Mirodatos C. A transient kinetic study of the carbon dioxide reforming of methane over supported Ru catalysts. Journal of Catalysis. 1999;184:202-12.
- [68] Shi C, Zhang P. Effect of a second metal (Y, K, Ca, Mn or Cu) addition on the carbon dioxide reforming of methane over nanostructured palladium catalysts. Applied Catalysis B: Environmental. 2012;115:190-200.
- [69] Safariamin M, Tidahy LH, Abi-Aad E, Siffert S, Aboukaïs A. Dry reforming of methane in the presence of ruthenium-based catalysts. Comptes Rendus Chimie. 2009;12:748-53.
- [70] Özkara-Aydınoğlu Ş, Özensoy E, Aksoylu AE. The effect of impregnation strategy on methane dry reforming activity of Ce promoted Pt/ZrO<sub>2</sub>. International Journal of Hydrogen Energy. 2009;34:9711-22.
- [71] Khani Y, Shariatinia Z, Bahadoran F. High catalytic activity and stability of ZnLaAlO<sub>4</sub> supported Ni, Pt and Ru nanocatalysts applied in the dry, steam and combined dry-steam reforming of methane. Chemical Engineering Journal. 2016;299:353-66.
- [72] El Hassan N, Kaydouh M, Geagea H, El Zein H, Jabbour K, Casale S, et al. Low temperature dry reforming of methane on rhodium and cobalt based catalysts: Active phase stabilization by confinement in mesoporous SBA-15. Applied Catalysis A: General. 2016;520:114-21.
- [73] Matsui N-o, Anzai K, Akamatsu N, Nakagawa K, Ikenaga N-o, Suzuki T. Reaction

- mechanisms of carbon dioxide reforming of methane with Ru-loaded lanthanum oxide catalyst. Applied Catalysis A: General. 1999;179:247-56.
- [74] Tsyganok AI, Inaba M, Tsunoda T, Hamakawa S, Suzuki K, Hayakawa T. Dry reforming of methane over supported noble metals: a novel approach to preparing catalysts. Catalysis Communications. 2003;4:493-8.
- [75] Alipour Z, Rezaei M, Meshkani F. Effect of alkaline earth promoters (MgO, CaO, and BaO) on the activity and coke formation of Ni catalysts supported on nanocrystalline Al<sub>2</sub>O<sub>3</sub> in dry reforming of methane. Journal of Industrial and Engineering Chemistry. 2014;20:2858-63.
- [76] Kim J-H, Suh DJ, Park T-J, Kim K-L. Effect of metal particle size on coking during CO<sub>2</sub> reforming of CH<sub>4</sub> over Ni–alumina aerogel catalysts. Applied Catalysis A: General. 2000;197:191-200.
- [77] Zhang M, Shengfu J, Linhua H, Fengxiang Y, Chengyue L, Hui L. Structural characterization of highly stable Ni/SBA-15 catalyst and its catalytic performance for methane reforming with CO<sub>2</sub>. Chinese Journal of Catalysis. 2006;27:777-81.
- [78] Jiang Z, Liao X, Zhao Y. Comparative study of the dry reforming of methane on fluidised aerogel and xerogel Ni/Al<sub>2</sub>O<sub>3</sub> catalysts. Applied Petrochemical Research. 2013;3:91-9.
- [79] Zhan Z, Barnett SA. An Octane-Fueled Solid Oxide Fuel Cell. Science. 2005:308:844-7.
- [80] Wang W, Ran R, Shao Z. Combustion-synthesized Ru–Al<sub>2</sub>O<sub>3</sub> composites as anode catalyst layer of a solid oxide fuel cell operating on methane. International Journal of Hydrogen Energy. 2011;36:755-64.
- [81] Zeng S, Zhang L, Zhang X, Wang Y, Pan H, Su H. Modification effect of natural mixed rare earths on Co/γ-Al<sub>2</sub>O<sub>3</sub> catalysts for CH<sub>4</sub>/CO<sub>2</sub> reforming to synthesis gas. International Journal of Hydrogen Energy. 2012;37:9994-10001.
- [82] Lyu Z, Wang Y, Zhang Y, Han M. Solid oxide fuel cells fueled by simulated biogas: Comparison of anode modification by infiltration and reforming catalytic layer. Chemical Engineering Journal. 2020:124755.

- [83] Zhao J, Xu X, Zhou W, Blakey I, Liu S, Zhu Z. Proton-Conducting La-Doped Ceria-Based Internal Reforming Layer for Direct Methane Solid Oxide Fuel Cells. ACS Applied Materials & Interfaces. 2017;9:33758-65.
- [84] Wang W, Zhou W, Ran R, Cai R, Shao Z. Methane-fueled SOFC with traditional nickel-based anode by applying Ni/Al<sub>2</sub>O<sub>3</sub> as a dual-functional layer. Electrochemistry Communications. 2009;11:194-7.
- [85] Hou Z, Yashima T. Small amounts of Rh-promoted Ni catalysts for methane reforming with CO<sub>2</sub>. Catalysis Letters. 2003;89:193-7.
- [86] García-Diéguez M, Pieta I, Herrera M, Larrubia M, Alemany L. RhNi nanocatalysts for the CO<sub>2</sub> and CO<sub>2</sub>+H<sub>2</sub>O reforming of methane. Catalysis Today. 2011;172:136-42.
- [87] Pawelec B, Damyanova S, Arishtirova K, Fierro JG, Petrov L. Structural and surface features of PtNi catalysts for reforming of methane with CO<sub>2</sub>. Applied Catalysis A: General. 2007;323:188-201.
- [88] Steinhauer B, Kasireddy MR, Radnik J, Martin A. Development of Ni-Pd bimetallic catalysts for the utilization of carbon dioxide and methane by dry reforming. Applied Catalysis A: General. 2009;366:333-41.
- [89] Menegazzo F, Signoretto M, Pinna F, Canton P, Pernicone N. Optimization of bimetallic dry reforming catalysts by temperature programmed reaction. Applied Catalysis A: General. 2012;439:80-7.
- [90] Lucrédio AF, Assaf JM, Assaf EM. Methane conversion reactions on Ni catalysts promoted with Rh: Influence of support. Applied Catalysis A: General. 2011;400:156-65.
- [91] Angeli SD, Monteleone G, Giaconia A, Lemonidou AA. State-of-the-art catalysts for CH<sub>4</sub> steam reforming at low temperature. International Journal of Hydrogen Energy. 2014;39:1979-97.
- [92] Bian Z, Das S, Wai MH, Hongmanorom P, Kawi S. A review on bimetallic nickel-based catalysts for CO<sub>2</sub> reforming of methane. ChemPhysChem. 2017;18:3117-34.
- [93] Wang C, Zhang Y, Wang Y, Zhao Y. Comparative Studies of Non-noble Metal

- Modified Mesoporous M-Ni-CaO-ZrO<sub>2</sub> (M= Fe, Co, Cu) Catalysts for Simulated Biogas Dry Reforming. Chinese Journal of Chemistry. 2017;35:113-20.
- [94] Ay H, Üner D. Dry reforming of methane over CeO<sub>2</sub> supported Ni, Co and Ni–Co catalysts. Applied Catalysis B: Environmental. 2015;179:128-38.
- [95] Gonzalez-delaCruz VM, Pereniguez R, Ternero F, Holgado JP, Caballero A. In situ XAS Study of Synergic Effects on Ni–Co/ZrO<sub>2</sub> Methane Reforming Catalysts. The Journal of Physical Chemistry C. 2012;116:2919-26.
- [96] Gao X, Tan Z, Hidajat K, Kawi S. Highly reactive Ni-Co/SiO<sub>2</sub> bimetallic catalyst via complexation with oleylamine/oleic acid organic pair for dry reforming of methane. Catalysis Today. 2017;281:250-8.
- [97] Wu T, Zhang Q, Cai W, Zhang P, Song X, Sun Z, et al. Phyllosilicate evolved hierarchical Ni-and Cu–Ni/SiO<sub>2</sub> nanocomposites for methane dry reforming catalysis. Applied Catalysis A: General. 2015;503:94-102.
- [98] Hua B, Yan N, Li M, Zhang Y-q, Sun Y-f, Li J, et al. Novel layered solid oxide fuel cells with multiple-twinned Ni<sub>0.8</sub>Co<sub>0.2</sub> nanoparticles: the key to thermally independent CO<sub>2</sub> utilization and power-chemical cogeneration. Energy & Environmental Science. 2016;9:207-15.
- [99] Jin C, Yang C, Zhao F, Coffin A, Chen F. Direct-methane solid oxide fuel cells with Cu<sub>1.3</sub>Mn<sub>1.7</sub>O<sub>4</sub> spinel internal reforming layer. Electrochemistry Communications. 2010;12:1450-2.
- [100] Ye X-F, Wang S, Wang Z, Xiong L, Sun X, Wen T. Use of a catalyst layer for anode-supported SOFCs running on ethanol fuel. Journal of Power Sources. 2008;177:419-25.
- [101] Zhan Y, Song K, Shi Z, Wan C, Pan J, Li D, et al. Influence of reduction temperature on Ni particle size and catalytic performance of Ni/Mg(Al)O catalyst for CO<sub>2</sub> reforming of CH<sub>4</sub>. International Journal of Hydrogen Energy. 2020;45:2794-807.
- [102] Frontera P, Macario A, Aloise A, Antonucci P, Giordano G, Nagy J. Effect of support surface on methane dry-reforming catalyst preparation. Catalysis Today. 2013;218:18-29.

- [103] Iulianelli A, Liguori S, Wilcox J, Basile A. Advances on methane steam reforming to produce hydrogen through membrane reactors technology: A review. Catalysis Reviews. 2016;58:1-35.
- [104] Li S, Gong J. Strategies for improving the performance and stability of Ni-based catalysts for reforming reactions. Chemical Society Reviews. 2014;43:7245-56.
- [105] Quang-Tuyen T, Shiratori Y, Sasaki K. Feasibility of palm-biodiesel fuel for a direct internal reforming solid oxide fuel cell. International Journal of Energy Research. 2013;37:609-16.
- [106] Wei T, Jia L, Zheng H, Chi B, Pu J, Li J. LaMnO<sub>3</sub>-based perovskite with in-situ exsolved Ni nanoparticles: a highly active, performance stable and coking resistant catalyst for CO<sub>2</sub> dry reforming of CH<sub>4</sub>. Applied Catalysis A: General. 2018;564:199-207.
- [107] Wang Z, Wang Z, Yang W, Peng R, Lu Y. Carbon-tolerant solid oxide fuel cells using NiTiO<sub>3</sub> as an anode internal reforming layer. Journal of Power Sources. 2014;255:404-9.
- [108] Yin Y, Li S, Xia C, Meng G. Electrochemical performance of IT-SOFCs with a double-layer anode. Journal of Power Sources. 2007;167:90-3.
- [109] Wang W, Zhu H, Yang G, Park HJ, Jung DW, Kwak C, et al. A NiFeCu alloy anode catalyst for direct-methane solid oxide fuel cells. Journal of Power Sources. 2014;258:134-41.
- [110] Wang W, Ran R, Shao Z. Lithium and lanthanum promoted Ni-Al<sub>2</sub>O<sub>3</sub> as an active and highly coking resistant catalyst layer for solid-oxide fuel cells operating on methane. Journal of Power Sources. 2011;196:90-7.
- [111] Wang W, Su C, Ran R, Shao Z. A new Gd-promoted nickel catalyst for methane conversion to syngas and as an anode functional layer in a solid oxide fuel cell. Journal of Power Sources. 2011;196:3855-62.
- [112] Wan T, Zhu A, Guo Y, Wang C, Huang S, Chen H, et al. Co-generation of electricity and syngas on proton-conducting solid oxide fuel cell with a perovskite layer as a precursor of a highly efficient reforming catalyst. Journal of Power Sources.

- 2017;348:9-15.
- [113] Gallego GS, Mondragón F, Barrault J, Tatibouët J-M, Batiot-Dupeyrat C. CO<sub>2</sub> reforming of CH<sub>4</sub> over La–Ni based perovskite precursors. Applied Catalysis A: General. 2006;311:164-71.
- [114] Moradi G, Rahmanzadeh M, Sharifnia S. Kinetic investigation of CO<sub>2</sub> reforming of CH<sub>4</sub> over La–Ni based perovskite. Chemical Engineering Journal. 2010;162:787-91.
- [115] Jahangiri A, Aghabozorg H, Pahlavanzadeh H, Towfighi J. Syngas Production from Reforming of Methane with CO<sub>2</sub> and O<sub>2</sub> over LaNi<sub>1-x</sub>Co<sub>x</sub>O<sub>3</sub> Perovskites. International Journal of Chemical Reactor Engineering. 2014;1.
- [116] Nair MM, Kaliaguine S, Kleitz F. Nanocast LaNiO<sub>3</sub> Perovskites as Precursors for the Preparation of Coke-Resistant Dry Reforming Catalysts. ACS Catalysis. 2014;4:3837-46.
- [117] Pereniguez R, Gonzalez-delaCruz VM, Caballero A, Holgado JP. LaNiO<sub>3</sub> as a precursor of Ni/La<sub>2</sub>O<sub>3</sub> for CO<sub>2</sub> reforming of CH<sub>4</sub>: Effect of the presence of an amorphous NiO phase. Applied Catalysis B: Environmental. 2012;123:324-32.
- [118] Zhang Z, Verykios XE, MacDonald SM, Affrossman S. Comparative study of carbon dioxide reforming of methane to synthesis gas over Ni/La<sub>2</sub>O<sub>3</sub> and conventional nickel-based catalysts. The Journal of Physical Chemistry. 1996;100:744-54.
- [119] Hua B, Li M, Luo J-l, Pu J, Chi B, Li J. Carbon-resistant Ni-Zr<sub>0.92</sub>Y<sub>0.08</sub>O<sub>2-δ</sub> supported solid oxide fuel cells using Ni-Cu-Fe alloy cermet as on-cell reforming catalyst and mixed methane-steam as fuel. Journal of Power Sources. 2016;303:340-6.
- [120] Meng X, Gong X, Yang N, Yin Y, Tan X, Ma Z-F. Carbon-resistant Ni-YSZ/Cu–CeO<sub>2</sub>-YSZ dual-layer hollow fiber anode for micro tubular solid oxide fuel cell. International Journal of Hydrogen Energy. 2014;39:3879-86.
- [121] Hua B, Li M, Pu J, Chi B, Jian L. BaZr<sub>0.1</sub>Ce<sub>0.7</sub>Y<sub>0.1</sub>Yb<sub>0.1</sub>O<sub>3-δ</sub> enhanced coking-free on-cell reforming for direct-methane solid oxide fuel cells. Journal of Materials Chemistry A. 2014;2:12576-82.
- [122] Gholami Z, Tišler Z, Rubáš V. Recent advances in Fischer-Tropsch synthesis using cobalt-based catalysts: a review on supports, promoters, and reactors. Catalysis

- Reviews. 2020:1-84.
- [123] Ghaffari Saeidabad N, Noh YS, Alizadeh Eslami A, Song HT, Kim HD, Fazeli A, et al. A Review on Catalysts Development for Steam Reforming of Biodiesel Derived Glycerol; Promoters and Supports. Catalysts. 2020;10:910.
- [124] Suiling L, Baitao L. Progress on the Catalysts for Carbon Dioxide Reforming of Methane to Synthesis Gas. Chemical Engineering of Oil & Gas. 2008;4.
- [125] Taufiq-Yap YH, Rashid U, Zainal Z. CeO<sub>2</sub>–SiO<sub>2</sub> supported nickel catalysts for dry reforming of methane toward syngas production. Applied Catalysis A: General. 2013;468:359-69.
- [126] Sengupta S, Deo G. Modifying alumina with CaO or MgO in supported Ni and Ni–Co catalysts and its effect on dry reforming of CH<sub>4</sub>. Journal of CO<sub>2</sub> Utilization. 2015;10:67-77.
- [127] Hao Z, Zhu Q, Jiang Z, Hou B, Li H. Characterization of aerogel Ni/Al<sub>2</sub>O<sub>3</sub> catalysts and investigation on their stability for CH<sub>4</sub>-CO<sub>2</sub> reforming in a fluidized bed. Fuel Processing Technology. 2009;90:113-21.
- [128] Rahemi N, Haghighi M, Babaluo AA, Jafari MF, Estifaee P. Synthesis and physicochemical characterizations of Ni/Al<sub>2</sub>O<sub>3</sub>–ZrO<sub>2</sub> nanocatalyst prepared via impregnation method and treated with non-thermal plasma for CO<sub>2</sub> reforming of CH<sub>4</sub>. Journal of Industrial and Engineering Chemistry. 2013;19:1566-76.
- [129] Munnik P, de Jongh PE, de Jong KP. Recent Developments in the Synthesis of Supported Catalysts. Chemical Reviews. 2015;115:6687-718.
- [130] Wei T, Qiu P, Jia L, Tan Y, Yang X, Sun S, et al. Power and carbon monoxide co-production by a proton-conducting solid oxide fuel cell with La<sub>0.6</sub>Sr<sub>0.2</sub>Cr<sub>0.85</sub>Ni<sub>0.15</sub>O<sub>3-δ</sub> for on-cell dry reforming of CH<sub>4</sub> by CO<sub>2</sub>. Journal of Materials Chemistry A. 2020;8:9806-12.
- [131] Wei T, Jia L, Luo J-L, Chi B, Pu J, Li J. CO<sub>2</sub> dry reforming of CH<sub>4</sub> with Sr and Ni co-doped LaCrO<sub>3</sub> perovskite catalysts. Applied Surface Science. 2020;506:144699. [132] Bitter J, Seshan K, Lercher J. Mono and bifunctional pathways of CO<sub>2</sub>/CH<sub>4</sub> reforming over Pt and Rh based catalysts. Journal of Catalysis. 1998;176:93-101.

- [133] Ferreira-Aparicio P, Rodriguez-Ramos I, Anderson J, Guerrero-Ruiz A. Mechanistic aspects of the dry reforming of methane over ruthenium catalysts. Applied Catalysis A: General. 2000;202:183-96.
- [134] Pan Y-X, Liu C-J, Shi P. Preparation and characterization of coke resistant Ni/SiO<sub>2</sub> catalyst for carbon dioxide reforming of methane. Journal of Power Sources. 2008;176:46-53.
- [135] Helveg S, Sehested J, Rostrup-Nielsen J. Whisker carbon in perspective. Catalysis Today. 2011;178:42-6.
- [136] Takenaka S, Kobayashi S, Ogihara H, Otsuka K. Ni/SiO<sub>2</sub> catalyst effective for methane decomposition into hydrogen and carbon nanofiber. Journal of Catalysis. 2003;217:79-87.
- [137] Rostrup-Nielsen JR. Catalytic Steam Reforming. Catalysis: Springer; 1984. p. 1-117.
- [138] Kuijpers E, Tjepkema R, Geus J. Elimination of the water-gas shift reaction by direct processing of CO/H<sub>2</sub>/H<sub>2</sub>O over Ni/SiO<sub>2</sub> catalysts. Journal of Molecular Catalysis. 1984;25:241-51.
- [139] Chen Y, deGlee B, Tang Y, Wang Z, Zhao B, Wei Y, et al. A robust fuel cell operated on nearly dry methane at 500° C enabled by synergistic thermal catalysis and electrocatalysis. Nature Energy. 2018;3:1042-50.
- [140] Zhao J, Xu X, Zhou W, Zhu Z. An in situ formed MnO–Co composite catalyst layer over Ni–Ce<sub>0.8</sub>Sm<sub>0.2</sub>O<sub>2-x</sub> anodes for direct methane solid oxide fuel cells. Journal of Materials Chemistry A. 2017;5:6494-503.

**Table 1** The application of OCRL materials in direct methane SOFCs.

OCRL	Method	Fuel	Anode support	Temperature (°C)	PPD (mW cm <sup>-2</sup> )	Durability (h)	Reference
Ni-Al <sub>2</sub> O <sub>3</sub>	GNP	CH <sub>4</sub>	Ni-SSZ	850	382	~2.5	[84]
Ni-TiO <sub>2</sub>	Sol-gel	$\mathrm{CH_4}$	Ni-YSZ	700	~230	~90	[107]
Ni-CeO <sub>2</sub>	Mixed mechanically	CH <sub>4</sub>	Ni-SDC	600	~160	~20	[108]
Ni-LDC	Sol-gel	$\mathrm{CH_4}$	Ni-SDC	650	671	~50	[83]
Ni-GDC	Mixed mechanically	CH <sub>4</sub> /CO <sub>2</sub>	Ni-YSZ	750	271	~45	[82]
$Ce_{0.9}Ni_{0.05}Ru_{0.05}O_2$	Precipitation	CH <sub>4</sub>	Ni-BZCYYb	500	370	~550	[139]
Co-MnO	Sol-gel	CH <sub>4</sub> /H <sub>2</sub> O	Ni-SDC	650	701	~15	[140]
NiFeCu-ZrO <sub>2</sub>	impregnation	CH <sub>4</sub> /O <sub>2</sub>	Ni-YSZ	650	334	~ 100	[109]
LiNaNi-Al <sub>2</sub> O <sub>3</sub>	GNP	CH <sub>4</sub> /CO <sub>2</sub>	Ni-SSZ	850	~530	-	[110]
		CH <sub>4</sub> /O <sub>2</sub>			538	-	
		CH <sub>4</sub> /H <sub>2</sub> O			~530	-	
GdNi-Al <sub>2</sub> O <sub>3</sub>	GNP	CH <sub>4</sub> /O <sub>2</sub>	Ni-YSZ	750	618	~7	[111]
		CH <sub>4</sub> /H <sub>2</sub> O		850	996	-	
		CH <sub>4</sub> /CO <sub>2</sub>		850	986	-	
NiCuFe-BZCYYb	Mixed mechanically	CH <sub>4</sub>	Ni-YSZ	800	1432	~12	[119]

NiCo-LDC	GNP	CH <sub>4</sub> /CO <sub>2</sub>	Ni-BZCYYb	700	910	~100	[98]
NiCo-SDC	Mixed mechanically	$\mathrm{CH_4}$	Ni-YSZ	800	350	7.5	[45]
LSCN@Ni	Sol-gel	CH <sub>4</sub> /CO <sub>2</sub>	Ni-BZCYYb	700	605	~65	[130]
Ni-La <sub>2</sub> O <sub>3</sub>	GNP	CH <sub>4</sub> /CO <sub>2</sub>	Ni-BZCY	700	120	~6	[112]
Cu-CeO <sub>2</sub> -YSZ	impregnation	CH <sub>4</sub>	Ni-YSZ	800	163	~30	[120]
Cu-MnO	Sol-gel	CH <sub>4</sub>	Ni-SDC	650	242	~60	[99]

GNP: glycine nitrate process